

# A practical model for simulating nonlinear behaviour of FRP strengthened RC beam-column joints

Javad Shayanfar<sup>a</sup> and Habib Akbarzadeh Bengar<sup>\*</sup>

Department of Civil Engineering, University of Mazandaran, Babolsar, Iran

(Received July 10, 2017, Revised January 26, 2018, Accepted January 30, 2018)

**Abstract.** Generally, beam-column joints are taken into account as rigid in assessment of seismic performance of reinforced concrete (RC) structures. Experimental and numerical studies have proved that ignoring nonlinearities in the joint core might crucially affect seismic performance of RC structures. On the other hand, to improve seismic behaviour of such structures, several strengthening techniques of beam-column joints have been studied and adopted in practical applications. Among these strengthening techniques, the application of FRP materials has extensively increased, especially in case of exterior RC beam-column joints. In current paper, to simulate the inelastic response in the core of RC beam-column joints strengthened by FRP sheets, a practical joint model has been proposed so that the effect of FRP sheets on characteristics of an RC joint were considered in principal tensile stress-joint rotation relations. To determine these relations, a combination of experimental results and a mechanically-based model has been developed. To verify the proposed model, it was applied to experimental specimens available in the literature. Results revealed that the model could predict inelastic response of as-built and FRP strengthened joints with reasonable precision. The simple analytic procedure and the use of experimentally computed parameters would make the model sufficiently suitable for practical applications.

**Keywords:** beam-column joint; nonlinear analysis; fiber-reinforced polymer (FRP); principal tensile stress; practical model

## 1. Introduction

Experimental and numerical studies as well as post-earthquake reconnaissance (Clyde *et al.* 2000, Pantelides *et al.* 2002, Calvi *et al.* 2002, Ghobarah and Said 2002, Ghobarah and El-Amoury 2005, Wong 2005, Kam 2010, Garcia *et al.* 2013, Niroomandi *et al.* 2014, Shayanfar and Akbarzadeh 2016a, Kheyroddin *et al.* 2016) proved that existing RC structures designed prior to current seismic code provisions with inadequate stirrup in the joint core, designed only for gravity load (lack of a capacity design principles) and insufficient seismic specific details (short lap splices, insufficient anchorage lengths and discontinuous longitudinal bars), are considerably vulnerable to shear or bond failure at beam-column joints during seismic actions. To improve seismic behaviour of such structures, several strengthening techniques of beam-column joints (epoxy repair, removal and replacement, prestressed and reinforced concrete jacketing, steel jacketing, haunch retrofit solution, steel fibers and externally bonding of fibre reinforced polymers (FRP)) have been studied and adopted in practical applications (Karayannis *et al.* 1998, Tsonos 2001, 2002a, Yurdakul and Avsar 2016, George *et al.* 2016, Campione *et al.* 2015,

Pampanin *et al.* 2006, 2007, Genesio 2012, Sharma 2013, Liu 2006, Antonopoulos and Triantafillou 2003, Parvin *et al.* 2010, Akguzel and Pampanin 2010, Akguzel 2011, Garcia *et al.* 2013, Del Vecchio *et al.* 2014, Truong *et al.* 2017). Among these strengthening techniques, the application of FRP materials has extensively increased, especially in case of exterior RC joints. Numerous investigations have been conducted to assess inelastic behaviour of RC joints strengthened using FRP materials which were categorized into three groups namely, experimental, numerical, and analytical studies.

In the group of experimental studies, Antonopoulos and Triantafillou (2003) tested exterior RC beam-column joints to assess the role of the various parameters (e.g., area fraction and distribution of FRP, applied axial load on column, transverse reinforcement in joint core, initial damage, carbon versus glass fibers, sheets versus strips, and the effect of transverse beams) on the shear capacity of strengthened specimens. The test results confirmed the important role of mechanical anchorages in limiting premature debonding. Parvin *et al.* (2010) tested exterior RC beam-column joints with inadequate shear and anchorage details. The test results revealed significant improvement in the shear capacity of the strengthened specimens. More importantly, the slippage of bottom longitudinal reinforcements of the beam into the joint core (bond failure) was considerably controlled via FRP strengthening system. Pampanin *et al.* (2007) and Akguzel and Pampanin (2010) tested non-seismically RC beam-column joints with 180°-hooks under varying axial load.

\*Corresponding author, Ph.D., Professor,

E-mail: [h.akbarzadeh@umz.ac.ir](mailto:h.akbarzadeh@umz.ac.ir)

<sup>a</sup> Post Graduate Student,

E-mail: [arch3d.ir@gmail.com](mailto:arch3d.ir@gmail.com)

The results showed that the proposed retrofit solution (including a U-shape horizontal laminate, wrapped around the exterior face of the tested specimens at the joint level) would prevent the expulsion of the concrete wedge mechanism and also improve the joint shear capacity. Del Vecchio *et al.* (2014) experimentally investigated nonlinear behavior of unconfined joints that did not conform to current seismic codes and also, the effectiveness of externally bonded fiber FRP as a strengthening technique. According to this study, the use of U-shaped uniaxial sheet wrapped also around the beam top side as a proper FRP joint core anchorage solution was capable of being a sound solution to avoid FRP end full debonding. It was also confirmed that the use of 0.4% as design maximum strain for FRP retrofit of a RC joint can be utterly conservative so that the maximum strain on FRP for test specimens was recorded more than 0.4%, with a maximum value of roughly 1.0%.

In the group of numerical studies, Parvin and Granata (2000), Parvin and Wu (2008), Mahini and Ronagh (2011), Dalalbashi *et al.* (2013), Eslami and Ronagh (2015), Akbarzadeh *et al.* 2015, Najafgholipour *et al.* (2017) proposed finite element models to evaluate nonlinear behaviour of FRP strengthened RC beam–column joint strengthened. The analyses results confirmed the effect of FRP sheets on the improvement of nonlinear response of RC beam – column joints. Niroomandi *et al.* (2010) evaluated the seismic performance of an RC frame strengthened by FRP sheets at beam-column joints. Flexural stiffness of FRP strengthened joints of the frame was first computed via nonlinear analyses of detailed finite element models of RC-joint–FRP materials. The positive effects of FRP sheets on moment–rotation relations of joints were then implemented into the numerical model of the frame through nonlinear link elements to carry out nonlinear static analysis on the FRP strengthened frame. The analysis results showed that seismic performance and seismic behavior factor of the FRP strengthened frame were considerably improved in comparison with the original frame. This approach was recently followed by Eslami *et al.* (2013), Ronagh and Eslami (2013), Hadigheh *et al.* (2014), Fakharifar *et al.* (2014), Akbarzadeh and Shayanfar (2015) Del Vecchio *et al.* (2016), to simulate the effect of FRP sheets at critical locations of beam-column joints at structural level. It should be noted that finite element method is not sufficiently practical enough to be followed by most engineers for modelling inelastic behavior of FRP strengthened joints at structural level from the point of view of time consuming and computational efforts. Moreover, due to various types of beam-column joints existing in a structure, this method becomes utterly impractical for the evaluation of seismic response of FRP strengthened frames.

Finally, in the group of analytical studies, Antonopoulos and Triantafillou (2002) and Al-Salloum and Almusallam (2007) developed analytical models to analyze exterior and interior RC joints strengthened using FRP materials, respectively, according to the model suggested by Pantazopoulou and Bonacci (1992). The models provided formulations to represent various stages of the response: concrete crushing, FRP rupture, FRP debonding and

yielding of the beam or column reinforcements. Akguzel and Pampanin (2012) simplified the aforementioned models using a combination of a mechanically-based model and empirical observations. An incremental procedure was developed to calculate shear capacity of a RC joint strengthened using FRP sheets. Bousselham (2010) proposed an analytical procedure to compute the principal tensile stress contributed by FRP sheets. The effective FRP strain is a key parameter in the model which was derived using empirical equations calibrated with database of experimental results. Del Vecchio *et al.* (2015) followed a similar approach but, a more refined calibration of the effective FRP strain was proposed to calculate the principal tensile stress and shear stress in the core of RC beam–column joints strengthened by FRP sheets. Hadi and Tran (2015) proposed a joint shear strength model for FRP strengthened joints based on average plane stress concept.

Reviewing the mentioned models (Antonopoulos and Triantafillou 2002, Al-Salloum and Almusallam 2007, Akguzel and Pampanin 2012), they does not seem to be sufficiently practical to compute FRP contribution in joint shear capacity. On the other hand, although the other analytical models (Bousselham 2010, Del Vecchio *et al.* 2015 and Hadi and Tran 2015) are practical enough to calculate the FRP effect on the joint core, the models do not give the corresponding joint shear deformation.

In order to assess nonlinear response of FRP strengthened RC structures, simulating the expected inelastic behavior in each member could be necessary. These behaviours include flexural or shear failure in columns and beams as well as shear or bond failure in the joint core before and after strengthening. However, in practice, the effects of shear failure in the joint core as well as other members on the seismic performance of RC structures are generally neglected in nonlinear analyses, especially for strengthened joints. In this paper, to simulate nonlinearities in the joint core and also consider shear behaviour beam or columns, before and after strengthening by FRP, practical models have been developed. The effect of FRP system on the joint core characteristics was determined via the principal stress criterion and according to a combination of a mechanically-based model and results reported by experimental studies on as-built and FRP strengthened joints. Overall, the simple analytic procedure and the use of experimentally computed parameters are capable of making the model sufficiently suitable for practical applications.

## 2. Proposed model for RC beam-column joints

Merely simulating inelastic behaviour in the beam/column elements along with considering the joint core as rigid according to the basic assumption that joint failure can be neglected in nonlinear analyses, might lead to quite misleading results (Sharma *et al.* 2011, Shayanfar *et al.* 2016). Moreover, For RC structures designed with insufficient stirrup in the joint core, seismic performance would inevitably be controlled by nonlinearities in the joint core. Accordingly, taking into account the effect of the joint

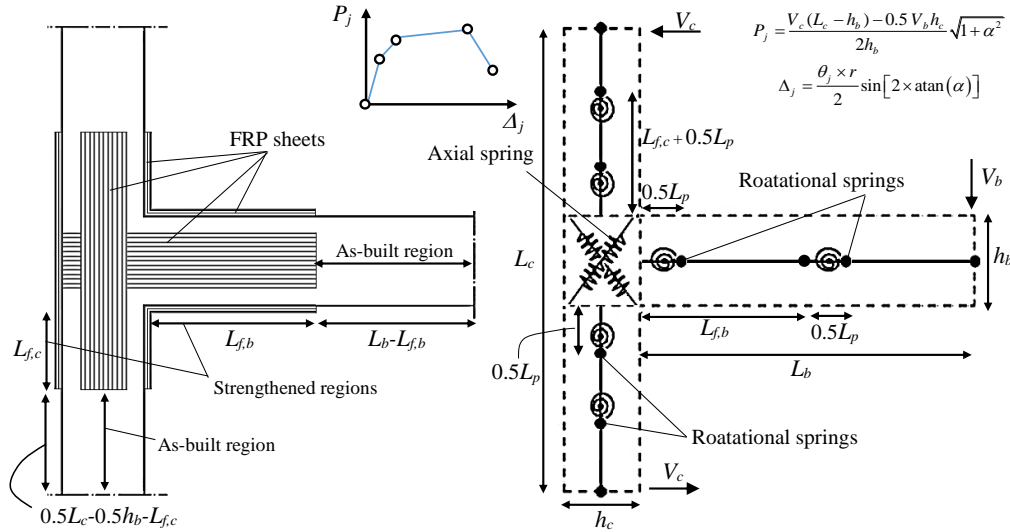


Fig. 1 Developed model for a FRP strengthened joint

core in nonlinear analyses is dramatically necessary. For simulating the joint region, various models have been recommended in literature (Biddah and Ghobarah 1999, Elmorsi *et al.* 2000, Pampanin *et al.* 2003, Lowes and Altoontash 2003, Shin and LaFave 2004, Mitra and Lowes 2007, Favvata *et al.* 2008, Sharma *et al.* 2011, Omidi and Behnamfar 2015, Shayanfar *et al.* 2016, O'Reilly and Sullivan 2017, De Risi *et al.* 2017). A numerical beam-column joint model including two shear springs and a flexural spring was proposed by Sharma *et al.* (2011) in which the characteristics of the springs were a function of principal tensile stress-shear deformation curve in the joint core. Omidi and Behnamfar (2015) proposed a numerical model consisting of a rigid offset element and beam and column elements with concentrated plasticity. The rigid offset element was calibrated to give a good estimation of initial stiffness according to the shear demand ratio of the connection. Two rotational springs in series, one for representing nonlinear behavior of beam and column elements and the other for containing the joint core effects, were taken into account in each of the beam and column elements with concentrated plasticity. Shayanfar *et al.* (2016) proposed a numerical model consisting of two diagonal axial springs in the joint core to simulate as-built RC beam-column joints. In this study, for FRP strengthened joints, this model has been extended to consider the effects of FRP sheets on inelastic behaviour of the joint core as well as beam and column elements as shown in Fig. 1. As can be seen, two rotational springs were defined in as-built and strengthened regions of beam/column elements. In current study, the sum of principal tensile stresses due to FRP and concrete contributions corresponding to each level of the joint rotation were then converted into axial force-displacement relation to be used in computing the characteristics of diagonal axial springs. After which, nonlinear analysis could be carried out to simulate as-built and FRP strengthened joints. It would also be useful to model FRP strengthened joints at structural level via commercial softwares based on lumped plasticity approach or simplified seismic assessment procedures such as

Tasligedik *et al.* (2016), Tasligedik (2017) and Del Vecchio *et al.* (2017).

### 3. Flexural and shear behavior in beam and column

In this section, the calculation of the rotational spring characteristics of beam and column in both as-built and strengthened regions will be presented. The effect of confinement on ductility of RC members due to FRP wrapping and stirrup have been proved by experimental tests (Wang and Restrepo 2001 and Kwan *et al.* 2015). In current paper, to determine the inelastic characteristics of the rotational springs, for the as-built and FRP strengthened regions, the confined concrete stress-strain relationships proposed by Mander *et al.* (1988) and Wang and Restrepo (2001) were followed, respectively. The cross section of an RC rectangular member can be classified into two zones: (i) unconfined concrete region; and (ii) effectively confined concrete region due to stirrup or FRP jacket. In this study, for easiness, instead of following a smeared concrete approach, a segmented core approach (Manfredi and Realfonzo 2001, Allington 2003, Akguzel and Pampanin 2012 and Akbarzadeh *et al.* 2016) was used in section analysis. Thus, the effectively confined region was assumed to be subjected to a uniform confining pressure due to lateral confinement provided by stirrups and FRP. After formulating the confined and unconfined concrete characteristics, based on the fiber analysis of the section, the moment-curvature relationship can be computed. Using obtained relationship, rotation in each level of curvature can be calculated based on the plastic hinge method proposed by Priestley *et al.* (1996) as 2

$$\theta_i = \frac{\varphi_i \times L}{2} \quad \text{for } \varphi_i < \varphi_y \quad (1a)$$

$$\theta_i = \frac{\varphi_y \times L}{2} + (\varphi_i - \varphi_y) \times L_{p,i} \quad \text{for } \varphi_i \geq \varphi_y \quad (1b)$$

in which

$$L_{p,i} = \frac{\varphi_i - \varphi_y}{\varphi_u - \varphi_y} L_p \geq 0 \quad (2)$$

where  $\theta_p$  = the plastic rotation;  $\varphi_y$  = the yield curvature;  $\varphi_u$  = the ultimate curvature;  $L$  = the clear span length;  $L_p$  defines the plastic hinge length which can be calculated based on the equation recommended by Pauley and Priestley (1992) as follows

$$L_p = 0.08L + 0.022f_y d_b \quad (3)$$

where  $f_y$  = the yield strength of longitudinal bars;  $d_b$  = the diameter of longitudinal bars. Under the action of seismic loading, initial flexural stiffness of an RC member crucially reduces due to the flexural cracks. Hence, the effective flexural stiffness of RC members,  $I_{eff}$ , should be used in nonlinear analysis. It can be calculated by

$$I_{eff} = \frac{M_y}{E_c \varphi_y} \quad (4)$$

where  $M_y$  = the yield moment;  $E_c$  = the elastic modulus of concrete. On the other hand, in order to take into account the effect of debonding failure in nonlinear analysis, FRP ultimate longitudinal strain was considered at least two values, FRP debonding strain,  $\varepsilon_{f,deb}$ , and rupture strain,  $\varepsilon_{f,u}$ . In current study, the fractural mechanics-based model of Holzenkampfer (1994) which has been slightly modified by Akguzel and Pampanin (2012), was used to determine the value of FRP strain debonding. According to this model, when debonding failure occurs in a FRP strengthened member,  $\varepsilon_{f,deb}$  can be expressed as

$$\varepsilon_{f,deb} = \frac{f_{f,deb}}{E_f} \quad (5)$$

where  $f_{f,deb}$  = the maximum tensile stress in FRP sheet corresponding to  $\varepsilon_{f,deb}$ . It can be calculated as

$$f_{f,deb} = c_1 \sqrt{\frac{0.5E_f f_c'}{t_f n_{fb}}}^{0.5} \quad \text{for } l_{bx} \geq l_{b,max} \quad (6)$$

in which ( $l_{bx}$  = the FRP development length)

$$l_{b,max} = \sqrt{\frac{E_f t_f}{0.5c_2 f_c'}^{0.5}} \quad (7)$$

where  $c_1$  and  $c_2 = 0.64$  and  $2$  as proposed by and Neubauer and Rostasy (1997) and Holzenkampfer (1994), respectively;

On the other hand, insufficient shear capacity in RC beams and columns is one of the most severe shortages of non-seismically detailed RC structures which is able to make them vulnerable against seismic actions (Lynn 2001, Sezen 2002, Elwood 2002). Accordingly, modelling of

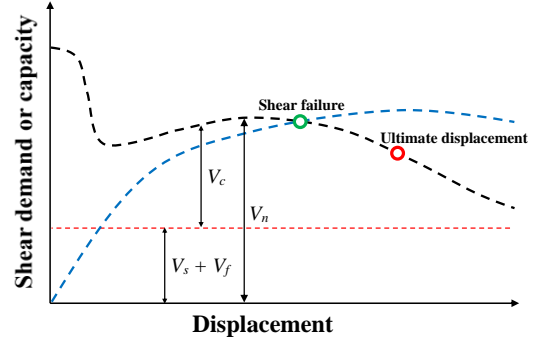


Fig. 2 Developed shear model

shear behaviour is required for a suitable nonlinear analysis. Experimental studies (Lynn 2001, Sezen 2002, Elwood 2002, Ho and Pam 2003, Moretti and Tassios 2007) indicated that shear capacity of RC beams and columns is a function of their inelastic flexural deformations. Furthermore, studies (Ghobarah and Galal 2004, Adhikary *et al.* 2004, Galal *et al.* 2005, Lee and Shin 2010, Del Zoppo *et al.* 2017) have been confirmed that wrapping FRP sheets could increase shear strength of RC members. To consider the effect of shear mechanism in evaluating RC member before and after strengthening, various models have been recommended in literature (Priestley *et al.* 1994, Triantafillou 1998, Sezen and Moehle 2004, Ghobarah and Galal 2004, Sung *et al.* 2005, Park *et al.* 2012, Shayanfar and Akbarzadeh 2016b). In current study, shear capacity was assumed as the sum of shear strengths due to concrete, stirrup and FRP as shown in Fig. 2. To determine the stirrup and FRP contributions, Eqs. (8) and (9) (Triantafillou 1998) were used as

$$V_s = \frac{A_v f_{yv} d}{s} \quad (8)$$

$$V_f = \rho_f E_f \frac{0.9}{\gamma_f} b d \varepsilon_{f,e} (1 + \cot \beta) (\sin \beta) \quad (9)$$

in which

$$\text{for } 0 \leq \rho_f E_f \leq 1$$

$$\varepsilon_{f,e} = 0.119 - 0.0205(\rho_f E_f) + 0.0104(\rho_f E_f)^2 \quad (10a)$$

$$\text{for } 0 \leq \rho_f E_f \leq 1$$

$$\varepsilon_{f,e} = -0.00065(\rho_f E_f) + 0.00245 \quad (10b)$$

$A_v$  = the total stirrup area in the beam/column;  $s$  = the centre to centre spacing of the stirrup;  $f_{yv}$  = the yield stress of the stirrup;  $d$  = the effective depth of cross-section. In current paper,  $A_e$  in Eq. (9) was taken into the account 80% of the total cross-section area ( $A_g$ ) (Priestley *et al.* 1994).  $\rho_f$  = FRP shear reinforcement ratio,  $\gamma_f$  = the coefficient accounting for FRP type,  $\beta$  = fiber inclination,  $E_f$  = the Young's modulus of the FRP composite material;  $b$  = the width of cross-section. According to ACI 440.2R (2002), for more than one type of shear reinforcement, the total

shear strength is limited as

$$V_f + V_s \leq 0.66\sqrt{f'_c}A_e \quad (11)$$

To calculate the concrete contribution in shear capacity,  $V_{con}$ , a simplified model was developed based on studies conducted by Park *et al.* (2012), Shayanfar and Akbarzadeh (2016b). Accordingly, assuming the shear resistance of intact concrete in the compression zone of section is considerably greater than the contributions of the aggregate interlock and dowel action (Park *et al.* 2012), shear capacity of concrete contribution can be written as

$$V_{con} = b \int_0^c v_{con}(x) dx \quad (12)$$

As shown in Fig. 3, an element of the section in the compression zone can be considered to be subjected to shear stress and compressive normal stress which would result principal compression and tension stresses. Consequently, when principal compression and tension stresses reach the material strength, the failure of material (concrete) would occur based on the Rankine's failure criteria (Chen 1982). Hence, using Mohr's circle approach and also taking into account the interaction between the principal compression and tension stresses in the element along with normal compressive stress in the compressive zone, the shear capacity can be written as

$$v_c(x) = \sqrt{f'_c [f'_c - f_c(x)]} \quad (13a)$$

controlled by compression

$$v_t(x) = \sqrt{f'_t [f'_t + f_c(x)]} \quad (13b)$$

controlled by tension

$$v_{con}(x) = \min[v_c(x), v_t(x)] \quad (14)$$

where  $f'_t$  = the tensile strength of concrete which was considered equal to  $0.292\sqrt{f'_c}$  (Park *et al.* 2006 and 2012).

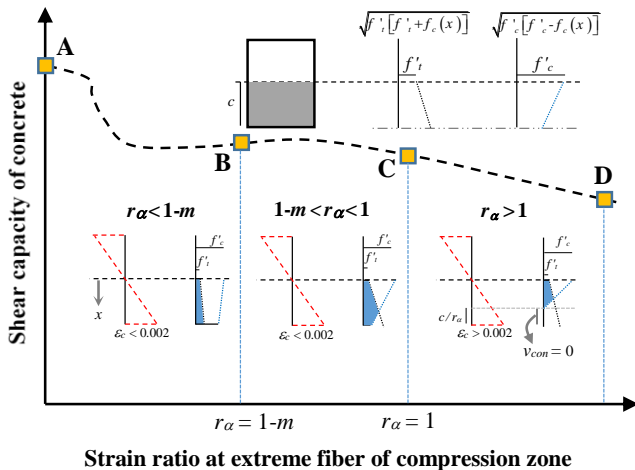


Fig. 3 Fluctuation of shear capacity with the increase of  $\varepsilon_c$

According to Eq. (14), the governing  $v_{con}$  at a location in the compression zone can be calculated corresponding to the smaller of the two shear stress capacities obtained from Eq. (13). It should be considered that in locations of the compression region which experiences compression softening,  $v_{con}(x_i)$  is equal to zero. On the other words, if compressive strain in concrete is higher than the strain at the peak compressive strength of concrete,  $v_{con}(x_i)$  can be neglected (Park *et al.* 2006). For simplify and solving the integral of the compression region, the compressive stress-strain relationship of the unconfined and confined concrete were assumed as an ascending branch of a second-order parabolic function to be reach at peak (Hognestad 1951, Park *et al.* 1982). As a result, the concrete stress-strain relationship can be determined as

$$f_c(\varepsilon) = F \left[ 2 \left( \frac{\varepsilon}{\varepsilon_1} \right) - \left( \frac{\varepsilon}{\varepsilon_1} \right)^2 \right] \quad \varepsilon \leq \varepsilon_1 \quad (15)$$

where  $F = f'_c$  and  $f'_{cc}$  for unconfined and confined concrete, respectively.  $\varepsilon_1 = \varepsilon_0$  and  $\varepsilon_{cc}$  for unconfined and confined concrete, respectively. Rearranging Eq. (15), we get

$$f_c(x) = F \left[ 2 \left( \frac{r_\alpha x}{c} \right) - \left( \frac{r_\alpha x}{c} \right)^2 \right] \quad x \leq c \quad (16)$$

where  $r_\alpha = \varepsilon_c / \varepsilon_1$ , normalized by  $\varepsilon_1$ . It is easily derived from Eqs. (13)-(16) that when normal stress  $f_c(x)$  is less than the value of  $F - f'_t$  which is corresponding to  $r_\alpha = 1 - m$  (where  $m = \sqrt{(F/f'_t)}$ ), the governing  $v_{con}$  would be determined as shear stress capacity controlled by tension. Otherwise, it can be controlled by both tension and compression.

Fig. 3 shows the distributions of the normal stress and shear stress capacity as a function of normal strain at the extreme compression fiber of the section,  $\varepsilon_c$ . Points A, B, C and D denote the initial state, the states at which the normal strain at extreme compression fiber reaches  $\varepsilon_0 \times (1 - m)$  and 1, and finally, the ultimate condition of moment-curvature analysis which can be determined based on Niroomandi *et al.* 2015, Shayanfar and Akbarzadeh 2016b), respectively. As a result, Eq. (12) can be rewritten as

$$V_{r_\alpha \leq 1-m} = b \int_0^c v_t(x) dx \quad (17)$$

$$V_{1-m \leq r_\alpha \leq 1} = b \int_0^{x=\frac{(1-m)c}{r_\alpha}} v_t(x) dx + b \int_{x=\frac{(1-m)c}{r_\alpha}}^c v_c(x) dx \quad (18)$$

$$V_{r_\alpha \geq 1} = b \int_0^{x=\frac{(1-m)c}{r_\alpha}} v_t(x) dx + b \int_{x=\frac{(1-m)c}{r_\alpha}}^{\frac{c}{r_\alpha}} v_c(x) dx \quad (19)$$

The shear capacity at each stage can be computed through adding the integration of shear stress capacities as

Table 1 Coefficients to compute shear capacity (Eq. (26))

$\varepsilon_c < 0.004$			$\varepsilon_c > 0.004$					
Strain ratio	$C_1$	$C_2$	$C_3$	Strain ratio	$C_1$	$C_2$	$C_3$	$C_4$
$r_\alpha \leq 1$	0.5	0.73	0.37	$r'_\alpha \leq 1$	0.5	0.73	0.37	-0.60
$1 - m \leq r_\alpha \leq 1$	0.4	0.75	-0.15	$1 - m \leq r'_\alpha \leq 1$	0.4	0.75	-0.15	-0.55
$r_\alpha \geq 1$	0.3	0.82	-1.00	$r'_\alpha \geq 1$	0.3	0.82	-1.00	-0.50

$$V_{r_\alpha \leq 1-m} = K_1 F_b \frac{c}{r_\alpha} \quad (20)$$

$$V_{1-m \leq r_\alpha \leq 1} = K_2 F_b \frac{c}{r_\alpha} \quad (21)$$

$$V_{r_\alpha \geq 1} = K_3 F_b \frac{c}{r_\alpha} \quad (22)$$

in which

$$K_1 = \frac{m}{2} \left[ \left\{ (m^2 + 1) \left[ a \sin\left(\frac{1}{\sqrt{m^2 + 1}}\right) + a \sin\left(\frac{r_\alpha - 1}{\sqrt{m^2 + 1}}\right) \right] \right\} \right. \\ \left. + \left\{ (r_\alpha - 1) \sqrt{m^2 + 2r_\alpha - r_\alpha^2} \right\} + m \right] \quad (23)$$

$$K_2 = \frac{1}{2} \left[ \left\{ -(r_\alpha - 1)^2 + m^2 \right\} + \right. \\ \left. \left\{ m(m^2 + 1) \left( a \sin\left(\frac{1}{\sqrt{m^2 + 1}}\right) + a \sin\left(\frac{-m}{\sqrt{m^2 + 1}}\right) \right) \right\} \right] \quad (24)$$

$$K_3 = \left\{ \frac{m}{2} (m^2 + 1) \left( a \sin\left(\frac{1}{\sqrt{m^2 + 1}}\right) + a \sin\left(\frac{-m}{\sqrt{m^2 + 1}}\right) \right) \right\} \\ + \frac{m^2}{2} \quad (25)$$

Fig. 4 shows the variation of shear capacity with the change in  $r_\alpha$ . As can be observed,  $c'$  and  $r_\alpha'$  are the neutral depth and the strain ratio at extreme compression fiber in the cross-section of the core concrete, respectively.

In order to derive a simplified shear strength model, for  $r_\alpha < 2$ , the effect of confinement in the core of the section was assumed to be ignored and subsequently, concrete in all location of the compression zone was taken into account as unconfined concrete. While for  $r_\alpha > 2$ , this effect was considered and, however, the contribution of the concrete cover was neglected in the determination of shear capacity because it spalls out when the normal strain at extreme compression fiber reaches 0.004. Accordingly, based on aforementioned assumptions and using regression analysis, Eqs. (20)-(22) were simplified as follows

for  $\varepsilon_c < 0.004$

$$V_{con} = C_f f'_c{}^{C_2} r_\alpha{}^{C_3} b c \quad (26a)$$

for  $\varepsilon_c > 0.004$

$$V_{con} = C_f f'_c{}^{C_2} r_\alpha{}^{C_3} b'' c' k^{C_4} \quad (26b)$$

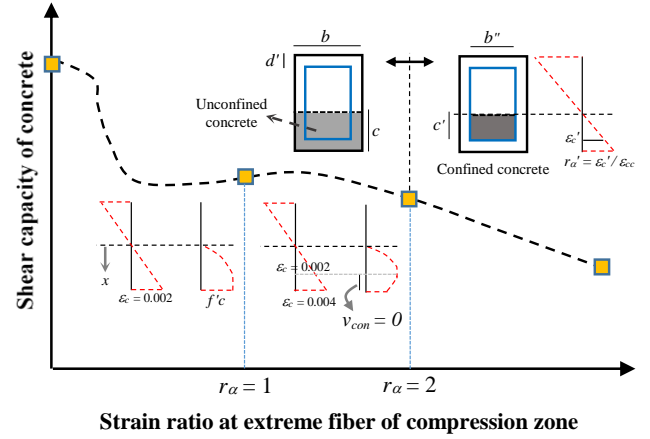


Fig. 4 Variation of shear capacity with the change in  $r_\alpha$

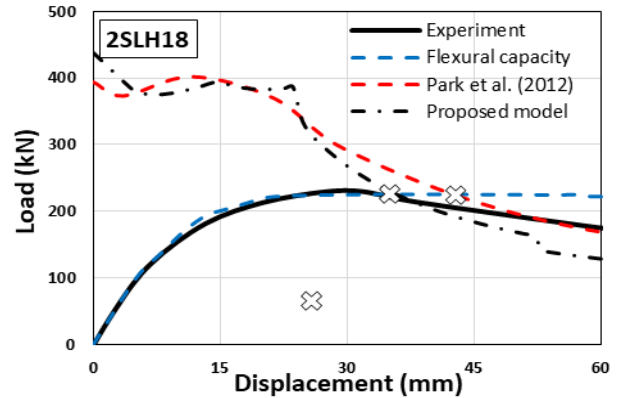


Fig. 5 Comparison between the simplified shear model and Park *et al.* (2012)'s model

As can be seen, the simplified shear strength is just a function of the geometry and material properties, neutral axis depth and strain ratio. Accordingly, the model seems to be practical enough to be used in shear assessment of RC members. To investigate the accuracy of the approximations used to develop the simplified shear model, in the Fig. 5, the developed shear model was compared to the shear model proposed by Park *et al.* (2012). For this, the specimen 2SLH18 of Lynn (2001) with failure mode as flexural-shear failure was chosen. As can be seen in the figure, the results obtained from the developed model were close to those determined by Park *et al.* (2012)'s model in terms of predicting shear strength and failure mode. Accordingly, as the proposed model is basically similar to Park *et al.* (2012), the accuracy of the approximations can be confirmed.

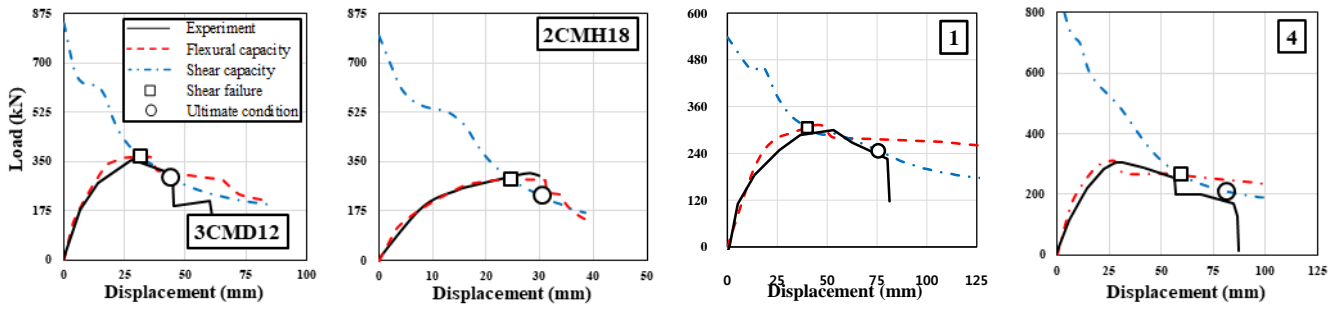


Fig. 6 Validation of the shear model against tests conducted by Lynn (2001) and Sezen (2002)

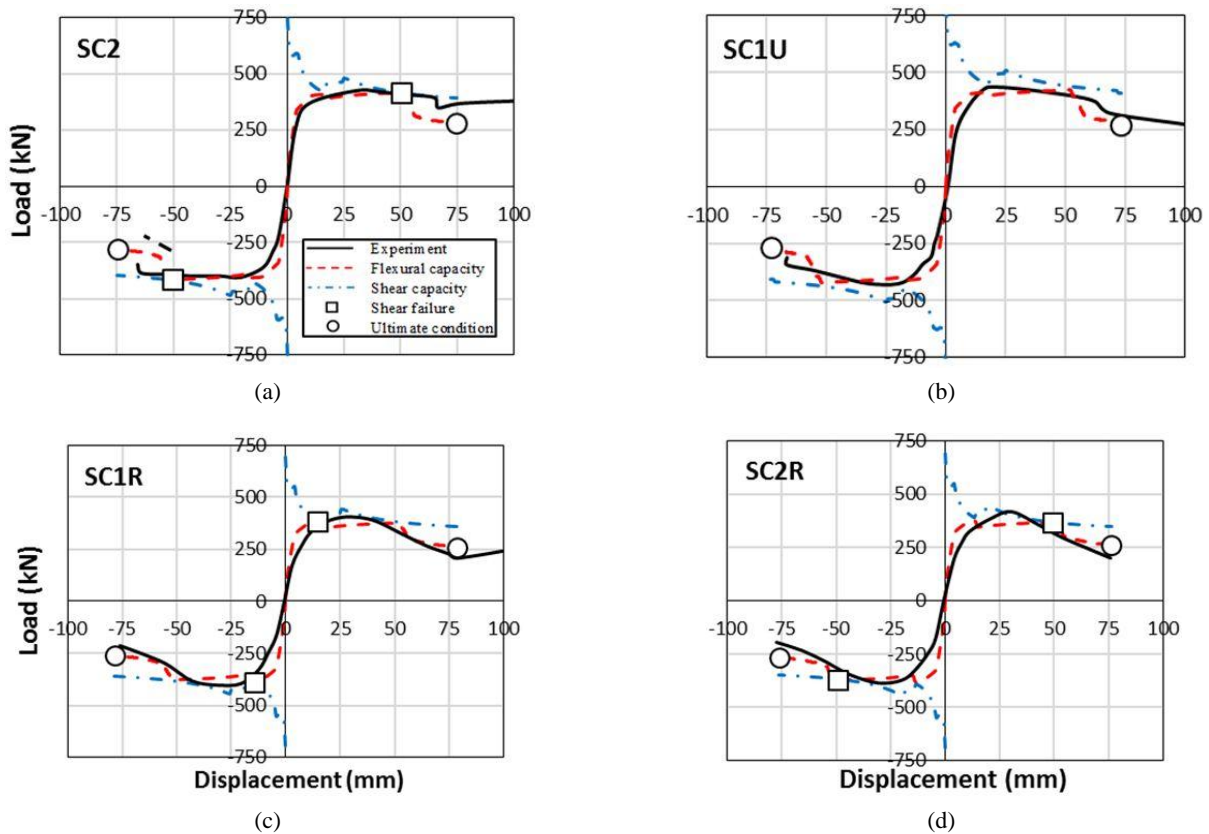


Fig. 7 Validation of the shear model against tests conducted by Ghobarah and Galal (2004) and Galal *et al.* (2005)

For a more extensive verification of the practical model, it was applied to experimental specimens. Lynn (2001) and Sezen (2002) conducted experimental studies on RC columns, with shear failure mode, subjected to cyclic loading. Complete detailed of the tested specimens can be found from Lynn (2001) and Sezen (2002). The load - displacement curves reported from the experiment were compared with those obtained from the practical model as shown in Fig. 6. It can be seen that the analytical and experimental results are in a reasonably good agreement. To eliminate brittle shear failure mode of short RC column using FRP wraps, Ghobarah and Galal (2004) and Galal *et al.* (2005) conducted experimental studies on FRP strengthened columns subjected to cyclic loading.

Complete detailed of the tested specimens can be found from Ghobarah and Galal (2004) and Galal *et al.* (2005). Fig. 7 compares the load - displacement curves reported

from the experiment with those obtained from the practical model. As can be observed, the model could estimate the lateral load-displacement relationship, shear strength and displacement capacity, all with reasonable accuracy. Note that, according the shear model is capable of predicting only initial failure mechanism, and after which, the member might indicate complicated post-failure modes, which can potentially be different from initial failure mechanisms. Accordingly, in Fig. 7, ultimate strength was regarded as maximum flexural capacity. Overall, according to Figs. (5)-(7), there is a good correlation between the experimental and analytical results, which confirms that the model is able to present reliable input data for the lumped plasticity approach. Furthermore, due to the fact that the shear model is utterly practical, it would be suitable for application in the current practice.

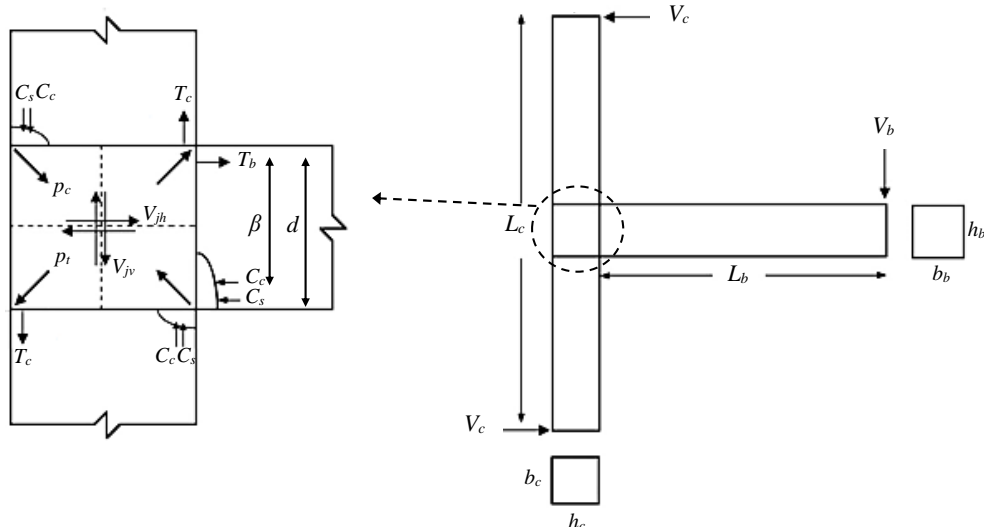


Fig. 8 Mechanics of an RC beam-column joint subjected to lateral loading

#### 4. Determination of the characteristics of diagonal axial springs

In order to compute the inelastic characteristics of the joint diagonal axial springs, the different methods such as conducting experimental tests, carrying out finite element analyses and developing an analytical method can be followed. However, experimental tests and finite element analysis methods do not seem practical in case of analyzing a structure with regard to the various types of beam-column joints that may be present in it. On the contrary, analytical methods are practical enough, for most engineers, to be applied in commercial software programs.

Fig. 8 indicates the mechanism of RC beam-column joints under seismic actions.  $L_b$  and  $L_c$  are the beam length measured from the column face and the total column height. The other parameters was defined in Fig. 8. Using the joint core equilibrium, the column shear force,  $V_c$ , can be written as

$$V_c = T_b - V_{jh} \quad (27)$$

where  $V_{jh}$  = the horizontal shear force acting on the joint core; Using the external equilibrium, the beam shear force,  $V_b$ , as a function of column shear force can be derived as

$$V_b = V_c \frac{L_c}{L_b + 0.5h_c} \quad (28)$$

Substituting Eq. (28) into Eq. (27), we get

$$V_b \frac{L_b + 0.5h_c}{L_c} = \frac{V_b L_b}{\beta_b} - V_{jh} \quad (29)$$

where  $\beta_b$  = the ratio of beam moment to tensile force adjacent to the joint core. Rearranging Eq. (29), we get

$$V_b = \frac{\beta_b \xi}{(\xi - \beta_b) L_b} V_{jh} \quad (30)$$

in which

$$\xi = \frac{L_c L_b}{L_b + 0.5h_c} \quad (31)$$

In this study, to convert  $V_b$  and  $V_c$  in each level of joint rotation,  $\theta_j$ , into axial force and displacement in the joint diagonal axial springs, the analytical procedure developed by Shayanfar *et al.* (2016) was used (the derivation of the equation was shown in Appendix A). It should be noted that the procedure is compatible to the commercial software SAP2000 (2008). Hence, axial force – displacement relation of the joint axial spring can be determined as follows

$$P_j = \frac{V_c (L_c - h_b) - 0.5 V_b h_c}{2h_b} \sqrt{1 + \alpha^2} \quad (32a)$$

$$\Delta_j = \frac{\theta_j \times r}{2} \sin(2 \times \text{atan}[h_b/h_c]) \quad (32b)$$

where  $\alpha$  = the joint aspect ratio;  $r$  = the length of diagonal of the joint core. The other parameters were defined in Fig. 8. To determine the accurate value of  $\beta_b$  corresponding to  $V_{jh}$ , iterative procedure is required but for simplicity, it was considered  $0.9d$  and  $0.85d$  for as-built and FRP strengthened joints. It should be noted that in case of strengthened joints with FRP sheets on the top and bottom of beam, FRP tension force at the column face is transferred into not only column but also, the joint core. Consequently,  $\beta_b$ , as the ratio of beam moment to tensile force increases with regard to the decrease of tension force. The available data do not clearly identify how much decrease occurs, but for simplicity, in current study,  $\beta_b$  was regarded as  $0.95d$  for the mentioned joints. Ultimately, as can be seen in Eq. (30), this equation is dependence on  $V_{jh}$ . Therefore, the determination of this parameter is required which will be explained in next section.

#### 4.1 Horizontal shear strength in the joint core

This section describes the determination of the value of  $V_{jh}$  in RC beam-column joint. For this, as the principal stress criterion considers axial stress entered by column axial load and is also adequately practical, it seems to be appropriate to provide a rational basis of determining joint horizontal shear strength. To determine  $V_{jh}$  using the principal stress criterion, an approach has been recommended by Priestley (1997) based on Mohr Theory which is given by

$$V_{jh} = \left( \sqrt{1 + \frac{f_v}{p_{t,tot}}} \right) p_{t,tot} b_j h_c \quad (33)$$

in which

$$b_j = \frac{b_b + b_c}{2} \quad (\text{Park and Mosalam 2012}) \quad (34)$$

As can be seen, the equation is a function of the total principal tensile stress,  $p_{t,tot}$ , in the joint core which can be calculated by (Akguzel and Pampanin 2012, Del Vecchio *et al.* 2015)

$$p_{t,tot} = p_{t,c} + p_{t,f} \quad (35)$$

where  $p_{t,c}$  and  $p_{t,f}$  define the principal tensile stress contributions of concrete and FRP, respectively.

#### 4.2 Concrete contribution in the joint core capacity

This section describes the determination of the value of principal tensile stress contribution due to concrete corresponding to maximum joint horizontal shear strength. To compute  $p_{t,c}$ , according to experimental evidence, limiting the principal tensile stress to values proportional to  $f_c$  has been recommended by Priestly (1997) (for joints with 90°-hooks bent into), Sharma *et al.* (2011) (for joints with 90°-hooks bent away and also, straight anchorage) and Akguzel and Pampanin (2012) (for joints with end-hook).

To investigate the capability of such limit states, they were compared with existing test results as shown in Fig. 9. The details of specimens were provided in Appendix B. Considering the values of the mean, coefficient of variation, CoV, and mean absolute percentage error, MAPE, they do not seem precise enough to be followed in accurately predicting joint capacity, although the models presents the advantages of being simple and efficiently practical.

Genesio (2012) proposed the limit states corresponding to first diagonal cracking and ultimate principle tension stresses including the effect of several parameters such as concrete strength, amount and detailing of beam bars, column axial load and geometric aspect ratio. Moreover, Sharma (2013) recommended that to consider the effect of joint aspect ratio, critical principal tensile stress values can be multiplied by the factor  $1/\alpha$ . According to existing test results, the principal tensile stress is not merely influenced by compressive strength of concrete, while the effects of joint aspect ratio, axial load level ( $N/A_c \times f_c$ ) and amount and detailing of beam bars might mainly be remarkable as shown in Fig. 10. As can be seen in the figure, increasing  $\alpha$  and beam reinforcement index ( $\rho_b f_{yb} / \sqrt{f_c}$ ), principle tensile stress would significantly decrease and increase, respectively. Increasing  $\alpha$ , the angle of the concrete strut with horizontal would be higher and consequently, the horizontal portion of the diagonal strut that resists the tensile force in beam bars could be less. Hence, for same tensile force, more compression force in the concrete strut would be required to maintain equilibrium. Because of the enhanced demand in the concrete strut, the joint shear capacity could reduce increasing in  $\alpha$ . The tension force in beam bars caused by the bending moment at the column face would be transferred into the joint core through the bond as well as the mechanical anchorage at the end of the beam bars. Considering that the shear failure in the joint core corresponds to the strut failure starting at the beam bar anchorage, it is argued that increasing  $r_B$  subsequently, an increase in the portion of tensile forces transferred by bond, the concrete strut would fail at a higher strength. Likewise, increasing  $\rho_b$ , the bending of the reinforcement will become more efficient in supporting the concrete strut (Genesio 2012). As can be seen in Fig. 10(c), experimental principle tensile stresses seem to be variable increasing  $r_N$ , even though the trend shows that  $p_{t,c} / \sqrt{f_c}$  marginally decrease increasing column axial load which it was confirmed according to Genesio (2012). It should be noted that the joint shear capacity would be improved increasing the level of the axial load applied on column based on the experimental studies conducted by Clyde *et al.* (2000) and Pantelides *et al.* (2002). The axial load can enhance the compression demand in the strut, while the strut width simultaneously increases by the expansion of the column compression zone. It can cause an increase in joint capacity. On the other hand, increasing applied axial load on column, tensile strains in column longitudinal bars is reduced which delays the column flexural yielding and also column bar yield penetration into the core of the joint. It would positively influence joint shear capacity.

In current study, according to experimental results (Appendix B), using regression analysis, the principal

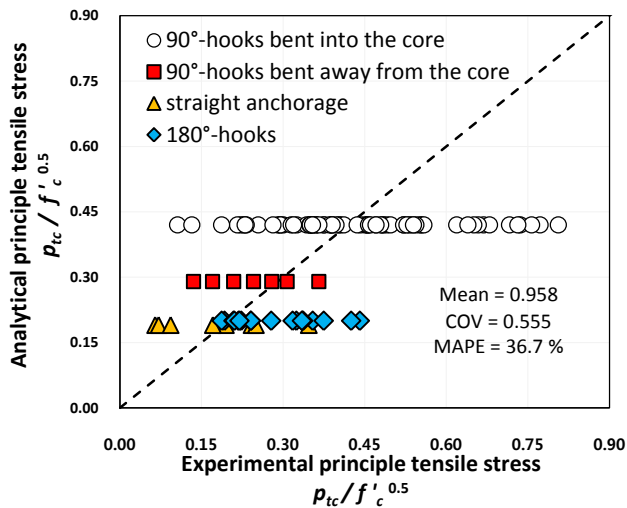


Fig. 9 Investigation of the capability of existing limit states

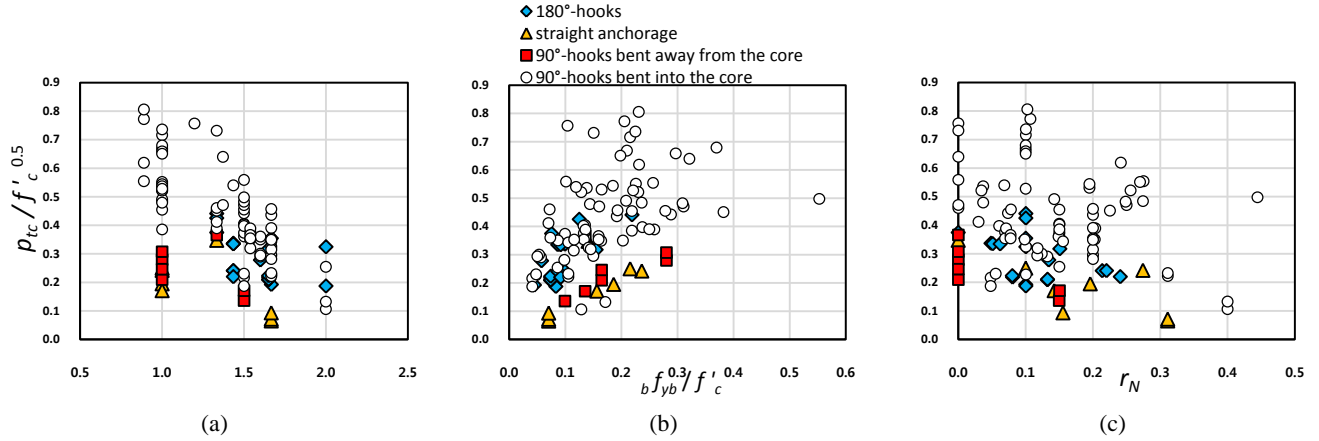


Fig. 10 Variations of experimental principle tensile stress in the joint core according to the geometry and material properties in experimental RC joints: (a) joint aspect ratio; (b) beam reinforcement index; (c) axial load level

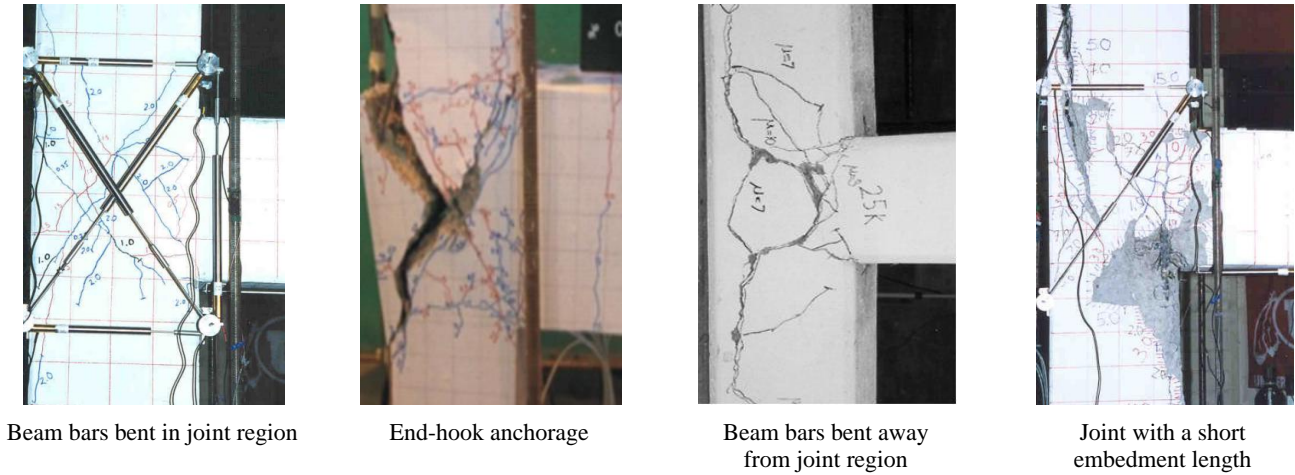


Fig. 11 Failure mechanisms of RC beam–column joint based on the experimental studies conducted by: (a) Pantalides *et al.* (2002); (b) Akguzel (2011); (c) Gergely *et al.* (2000); (d) Pantalides *et al.* (2002)

tensile stress contribution due to concrete corresponding to maximum joint horizontal shear strength was proposed as

$$p_{t,c} = \frac{\omega_1 \omega_2}{\alpha_{setup}} \sqrt{f'_c} \quad (36)$$

in which

$$\omega_1 = 1.986X^{0.339} - 1.232 \quad (37)$$

$$X = (1 + r_N)^{-1.26} f'_c{}^{0.08} r_B^{0.26} \alpha^{-0.42} \times \left(\frac{h_b}{b_b}\right)^{-0.08} \left(\frac{b_b}{b_c}\right)^{-0.08} \geq 0.3 \quad (38)$$

where  $\omega_2$  = the coefficient of the anchorage type of beam longitudinal bars; Experimental and analytical studies (Priestley 1997, Murty *et al.* 2003, Parvin *et al.* 2010, Akguzel and Pampanin 2012, Sharma *et al.* 2011, Hassan 2011, Shafaei *et al.* 2014, Shayanfar *et al.* 2016) confirmed that failure mechanism of RC joints is a function of the

anchorage type of beam longitudinal bars as shown in Fig. 11. As can be seen in Fig. 11(a), for joints with beam bars bent in, since the diagonal struts in the joint core would be stabilized, after the first diagonal crack, the joint would be capable of further resistance and subsequently, a hardening behaviour can be assumed until the principal tensile stress reaches its maximum value,  $p_{t,c}$  corresponding to more severe diagonal cracking and damage in the joint core. For joints with end-hook anchorage, failure mechanism is utterly different from joints with beam bars bent in. After the first diagonal crack, nonlinear behaviour of joints would lead to a particular “concrete wedge” brittle failure mechanism (Pampanin *et al.* 2002), due to the interaction between shear cracking and stress concentration at the hook anchorage location (Fig. 11(b)). It confirms the inefficiency of alternative shear transfer mechanism in the joint core, after first cracking, when beam bars are anchored as end-hook. As a result, maximum joint strength occurs corresponding to first cracking. Again for joints with beam bars bent away from joint core, the failure mechanism is virtually similar to end hook joints. In this anchorage type of joints, due to the fact that the first diagonal crack

propagates along the beam bars bent out of the joint and also due to the lateral thrust, the cover to column cover would be fractured (Fig. 11(c)). Therefore, the diagonal struts in the joint cannot also be stabilized and subsequently, the joint failure is expected at early stage compared to joints with beam bars bent in. The reason why in joints with 90°-hooks bent away from the core or end hooks, the development of a hardening behaviour would not be possible because an effective node to active the diagonal compression strut cannot be provided. In case of joints in which beam bars terminates in the joint core with a short embedment length, the bond mechanism between concrete and beam bars becomes the critical parameter. The crack starts at the end of the straight anchorage nearly at the mid-depth of the column (Fig. 11(d)). It may induce the bond failure much before the diagonal compressive strut mechanism could be fully developed. As a result, maximum joint strength occurs by far lower than that of joints with beam bars bent in. In current study, based on an analyze on test specimens available in literature, to consider the effect of anchorage type of beam bars, the parameter  $\omega_2$  was defined which is equal to  $\omega_2 = 0.85, 0.42$  and  $0.41$  for joints with end hooks, 90°-hooks bent away from the core and straight anchorage, respectively.

In general, two different setups are used for the testing of exterior joints in which (1) a concentrated load ( $V_b$ ) is vertically applied into at the beam tip and the column is hinged at the bottom and top ends (type 1); (2) the joint is horizontally loaded at the top column tip and is free to move in the horizontal direction. Moreover, the beam and bottom column are hinged (type 2). Although the used static systems are equivalent for the loading of the beam-column joint, the deformation shapes are quite different. In general, the results extracted from experiments (i.e., principle tensile stress) are taken into account identical for both types of test setups. However, according to the finite element study conducted by Genesio (2012), the nonlinear characteristics of an RC joint would dramatically be affected by the type of joint test. Consequently, the factor of  $\alpha_{setup}$  was defined to convert results from a test setup to another. In this study,  $\alpha_{setup} = 1.18$  (Genesio 2012) were used for converting joints with test type 1 into test type 2 ( $\alpha_{setup} = 1$  for test type 2). It is noteworthy that the boundary condition in the test type 1

is closer to the reality of a moment resisting frame for deformation shape. Therefore, at structural level, in order to follow the aforementioned maximum principal tensile stress in the determination of the nonlinear characteristics of joint core, it should be divided by  $\alpha_{setup}$ .

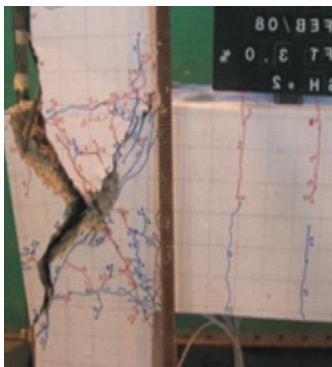
### 4.3 FRP contribution in the joint core capacity

This section addresses the determination of the value of principal tensile stress contribution due to FRP corresponding to maximum joint horizontal shear strength. As it was discussed, for as-built RC beam-column joints, except joints with 90°-hooks bent into, the effective node point would not be provided in the joint core to develop diagonal compression strut mechanism. According to experimental studies (Parvin *et al.* 2010, Akguzel 2011), FRP system is capable of changing in failure mechanism so that the joints would fail similar to joints with 90°-hooks and to more severe diagonal cracking and damage in the joint core can be expected (Fig. 12). Accordingly, for joints with 90°-hooks bent out, 180°-hooks and straight anchorage,  $p_{t,c}$  might increase and if in a FRP retrofit scheme, the effective node points are perfectly provided to develop diagonal compression strut mechanism,  $\omega_2$  could ideally be assumed equal to 1. As a result, based on Eq. (36), the principal tensile stress contribution due to concrete corresponding to maximum joint horizontal shear strength can be rewritten for FRP strengthened joints

$$p_{t,c} = \frac{\omega_1 \omega_2}{\alpha_{setup}} \sqrt{f'_c} \times \left[ \frac{1 - (1 - \omega_2)(1 - \psi)}{\omega_2} \right] \quad (39)$$

where  $\psi$  = the coefficient to consider the change in the joint failure mechanism. In current study, to be conservative and simple, for all type anchorage of beam bars,  $\psi$  was assumed equal to 25%.

According to the analytical studies conducted by Bousselham (2010), Del Vecchio *et al.* (2015), the principal tensile stress contributions due to FRP in a generic direction can be calculated based on the tensile stress in the FRP system ( $E_f \times \epsilon_{f,e}$ )



(a) As-built joint



(b) FRP strengthened joint

Fig. 12 Damage state of the joint core before and after strengthening by FRP system: (a) specimen 2D1; (b) specimen 2D3 (note: the tests were conducted by Akguzel (2011))

$$p_{t,f} = \frac{A_{f,eq} E_f \varepsilon_{f,e}}{b_j h_b} \sin \theta \quad (40)$$

where  $\theta$  = the direction of the principal tensile stresses which was taken into account equal to a  $\tan(h_b/h_c)$  corresponding to maximum joint strength (Paulay and Priestley 1992, Bousselham 2010, Del Vecchio *et al.* 2015) (nearly correct if an effective node point was provided to develop diagonal compression strut mechanism);  $E_f$  = the Young's modulus of FRP fibers;  $\varepsilon_{f,e}$  = the effective FRP strain;  $A_{f,eq}$  = the equivalent FRP area on the joint core which can be computed based on Del Vecchio *et al.* (2015):

- (a) Uniaxial fabric with fibers in the direction of beam axis ( $0^\circ$ ) or column axis ( $90^\circ$ ):

$$A_{f,eq} = n_l n_s t_f h_b \sin \theta \quad \text{for } \beta = 0^\circ \quad (41a)$$

$$A_{f,eq} = n_l n_s t_f h_c \cos \theta \quad \text{for } \beta = 90^\circ \quad (41b)$$

- (b) Bidirectional fabric with fibers in the direction of beam and column axes ( $0^\circ, 90^\circ$ )

$$A_{f,eq} = n_l n_s t_f h_c \cos \theta (1 + \tan^2 \theta) \quad (41c)$$

- (c) Quadriaxial fabric with any fibers in the direction of beam ( $0^\circ$ ) and column ( $90^\circ$ ) axes and  $\pm 45^\circ$

$$A_{f,eq} = n_l n_s t_f h_c \cos \theta (1 + \tan \theta + 2 \tan^2 \theta) \quad (41d)$$

where  $n_s$  = the number of joint core sides strengthened by FRP systems in the plane of the load;  $n_l$  = the number of FRP layers;  $t_f$  = the thickness of the FRP sheets;  $\beta$  = the inclination of joint core FRP fibers. As can be seen in Eq. (40), FRP contribution is a function of the effective FRP strain.

#### 4.3.1 Effective FRP strain

In this section, a practical formulation will be expressed in order to calculate the effective FRP strain,  $\varepsilon_{f,e}$ , in a generic direction corresponding to the maximum joint shear capacity and subsequently, to compute FRP contribution by Eq. (40). In this study, a large database of test specimens was provided based on FRP strengthened specimens with failure mode as joint shear failure or FRP debonding or FRP tensile failure. The properties of test specimens were shown in Appendix C. Experimental FRP strain corresponding to the maximum joint shear capacity was calculated through Eq. (42).

$$\varepsilon_{f,e}^{\text{exp}} = \frac{p_{t,f}^{\text{exp}} b_j h_b}{A_{f,eq} E_f \sin \theta} \quad (42)$$

in which

$$p_{t,f}^{\text{exp}} = p_{t,tot}^{\text{exp}} - p_{t,c} \quad (43)$$

$$p_{t,tot}^{\text{exp}} = \sqrt{\left(\frac{f_v}{2}\right)^2 + (v_{jh}^{\text{exp}})^2} - \frac{f_v}{2} \quad (44)$$

$$v_{jh}^{\text{exp}} = \frac{(\xi - \beta_b) L_b V_b^{\text{exp}}}{\beta_b \xi b_j h_c} \quad (45)$$

where  $p_{t,tot}^{\text{exp}}$  and  $v_{jh}^{\text{exp}}$  define the total principle tensile stress and shear stress extracted from experiments due to concrete and FRP contributions, respectively. It is worth adding that for experimental joints with a concentrated load in the column tip, the experimental shear force at the beam tip,  $V_b^{\text{exp}}$ , can be determined using Eq. (45). Based on the experimental results, the effective strain in FRP sheets corresponding to the maximum strength of the joint core can be determined using regression analysis as

$$\varepsilon_{f,e} = 0.235 X^{-1.4} \leq 0.01 \quad (46)$$

in which

$$X = C_{I,D} C_{M,A} \times \omega \quad (47)$$

$$\omega = (A_{f,eq} E_f)^{0.5} \times \left(\frac{h_b}{b_b}\right)^{-1.5} \times (1 + r_N)^{-3.9} \times f_c^{-1.3} \times r_B^{-0.45} \times \alpha^{-2.05} \quad (48)$$

According to experimental results (Antonopoulos and Triantafillou 2003, Garcia *et al.* 2013), if the FRP retrofitting system was applied on damaged joint core, it could cause a decrease in joint capacity compared to applying retrofitting system on an undamaged joint. On the other hand, experimental results (Antonopoulos and Triantafillou 2003, Ghobarah and El-Amoury 2005, Parvin *et al.* 2010, Le-Trung *et al.* 2010, Del Vecchio *et al.* 2014) indicated that mechanically anchorage of FRP sheets (i.e., using wrapped FRP sheets on the adjacent beams or columns) can improve joint capacity. Accordingly, to

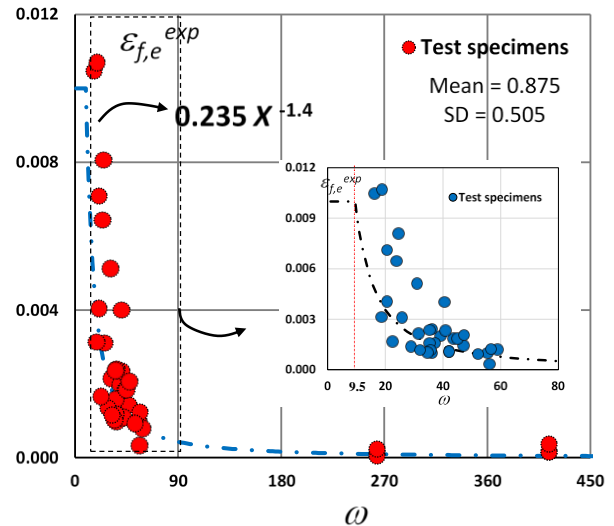


Fig. 13 Variation of FRP effective strain as a function of  $\omega$

consider these effects in the model, the coefficients  $C_{I.D.}$  and  $C_{M.A.}$  were defined which can be calculated corresponding to values proposed by Del Vecchio *et al.* (2015).  $C_{I.D.}$  is 0.8 and 1 for cracked and undamaged joint core,  $C_{M.A.}$  is 1.5 and 1 for with and without mechanical anchorage of the joint core FRP sheets. Fig. 4 shows the variation of the effective strain in FRP sheets corresponding to the maximum strength of the joint core as a function of  $X$ . As can be observed, increasing value  $\omega$ , the trend  $\epsilon_{f,e}^{ex}$  would considerably decrease, especially, for  $\omega$  higher than 50 which  $\epsilon_{f,e}^{exp}$  is estimate lower than 0.001.

The values of the mean and standard deviation, SD, of the ratio of the FRP effective strain obtained-to-experimental are 0.867 and 0.504, respectively. Considering these values, it can be concluded that the proposed effective strain conservatively predicts the FRP effective strain obtained from experiments.

Fig. 14 illustrates the variations of concrete and FRP contribution in the total principle tensile stress in the test specimen of Del Vecchio *et al.* (2014) for a range of axial load index, joint aspect ratio and the number of FRP layers. The selected specimen was T\_FL1, which was strengthened with one layer of quadriaxial carbon fibers, CFRP, ( $n_l = 1$ ) applied to the joint core and slightly extended to the beams nearly 200 mm. Panel strengthening was anchored through uniaxial U-shaped CFRP wraps on the beam ends for 200 mm ( $C_{I.D.} = 1$  and  $C_{M.A.} = 1.5$ ). Quadriaxial CFRP sheets with thickness of 0.053 mm, Young's modulus of 230 GPa and ultimate strain of 1.5% were used for joint panel strengthening. No shear reinforcement was placed in the joint core and beam bars were anchored with 90°-hooks bent into the joint.  $\alpha$  and  $r_N$  were equal to 1.67 and 0.2, respectively. Complete detailed of the tested specimen can be found from Del Vecchio *et al.* (2014). As can be seen in Fig. 14(a), according to the proposed model, total principle tensile stress is varied increasing  $r_N$ . Although  $p_{t,c}$  as a function of axial load drops roughly 50% for a range  $r_N$ , from 0 to 0.45, conversely, that of for FRP contribution increase for the same. This increase can also be confirmed by the incremental procedure developed by Akguzel and Pampanin (2012) in which  $p_{t,f}$  is positively influenced by an increase in the axial load level. In Fig. 14(b), the effect of joint aspect ratio on principle tensile stress in the joint core

was investigated. The trends are virtually similar to the trends for the variation of  $r_N$ . Since  $A_{f,eq}$  is significantly dependence on  $\tan(\alpha)$  and FRP effective strain would also enhance through increasing  $\alpha$ , it was expected that  $p_{t,f}$  experienced a spectacular increase. A closer look reveals that it compensates considerable decrease  $p_{t,c}$  being adversely influenced by increasing  $\alpha$  so that at nearly  $\alpha = 1.4$ ,  $p_{t,tot}$  was predicted to reach 2.2 MPa, where  $\alpha = 2$ , an approximately 26 percent leap. In Fig. 14(c), two type of the FRP strengthening system were compared.  $p_{t,f2}$  denotes a FRP strengthened joint which was assumed to be strengthened with uniaxial CFRP in both direction of beam and column axes. Other characteristics of the joint were considered to be similar to specimen T\_FL1. As can be observed, in the joint strengthened by quadriaxial fabrics, FRP contribution in principle tensile stress is by far more than the joint strengthened by uniaxial CFRP fabrics, roughly 90%. Accordingly, it can be confirmed that quadriaxial fabrics (or fibers inclined at 45°), which are commonly used in the design practice, would also be by far more effective than joint strengthening systems with FRP sheets in both the longitudinal and transverse directions.

#### 4.3.2 Principal tensile stress–joint rotation relation of FRP strengthened joints

In this section, the determination of the principal tensile stress - joint rotation relation for FRP strengthened joints with various anchorages of beam bars in the joint core will be explained. In current paper, based on the analytical studies conducted by Hassan (2010), Sharma *et al.* (2011) and Shayanfar *et al.* (2016), the effects of the bond-slip mechanism were indirectly taken into account in nonlinear analysis so that adding the joint rotation due to beam bar slip,  $\theta_{slip}$ , to joint shear deformation,  $\gamma_j$ , the rotation of the joint core can be determined ( $\theta_j = \gamma_j + \theta_{slip}$ ). In this paper, for FRP strengthened joints with various anchorages of beam bars, the principal tensile stress - joint rotation relations were developed based on the experimental studies conducted by Antonopoulos and Triantafillou (2003), Parvin *et al.* (2010), Akguzel and Pampanin (2010) and Garcia *et al.* (2013) as shown in Fig. 15. Here,  $K_{deg}$  defines the post-peak stiffness. for FRP strengthened joints with 90°-hooks and other anchorage types,  $K_{deg}$  and  $\theta_i$  were

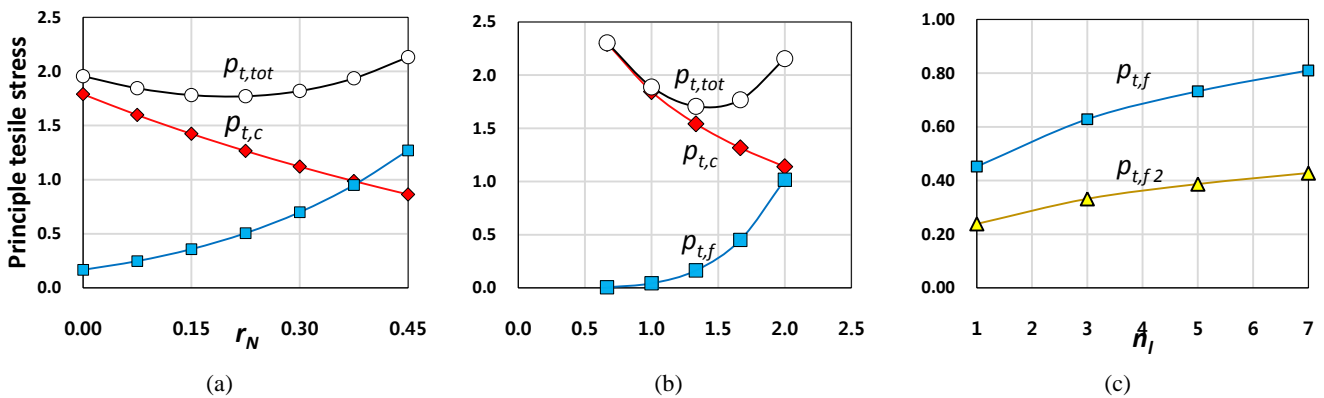


Fig. 14 Variations of principle tensile stress in the test specimen of Del Vecchio *et al.* (2014): (a) axial load index; (b) joint aspect ratio; (c) the number of FRP layers

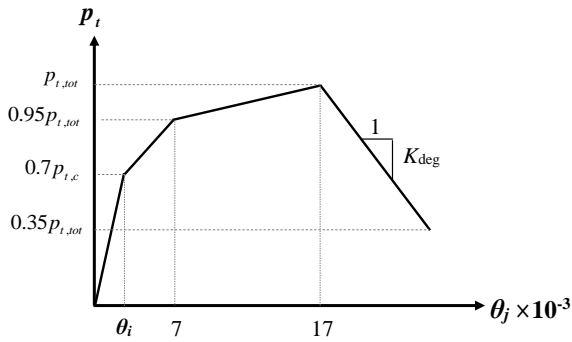


Fig. 15 Proposed principal tensile stress-joint rotation relations for FRP strengthened joints

taken into account -80 and -85 (MPa/rad) and 0.001 and 0.0015 radian, respectively. It should be noted that similarly, Shayanfar *et al.* (2016) recommended the appropriate strength degradation curves.

4.3.3 Principal tensile stress–joint rotation relation of FRP strengthened joints

In this section, the determination of the principal tensile stress - joint rotation relation for FRP strengthened joints with various anchorages of beam bars in the joint core will be explained. In current paper, based on the analytical studies conducted by Hassan (2010), Sharma *et al.* (2011) and Shayanfar *et al.* (2016), the effects of the bond-slip mechanism were indirectly taken into account in nonlinear analysis so that adding the joint rotation due to beam bar slip,  $\theta_{slip}$ , to joint shear deformation,  $\gamma_j$ , the rotation of the joint core can be determined ( $\theta_j = \gamma_j + \theta_{slip}$ ). In this paper, for FRP strengthened joints with various anchorages of beam bars, the principal tensile stress - joint rotation relations were developed based on the experimental studies conducted by Antonopoulos and Triantafillou (2003), Parvin *et al.* (2010), Akguzel and Pampanin (2010) and Garcia *et al.* (2013) as shown in Fig. 15. Here,  $K_{deg}$  defines the post-peak stiffness. for FRP strengthened joints with 90°-hooks and other anchorage types,  $K_{deg}$  and  $\theta_i$  were taken into account -80 and -85 (MPa / rad) and 0.001 and 0.0015 radian, respectively. It should be noted that similarly, Shayanfar *et al.* (2016) recommended the appropriate strength degradation curves.

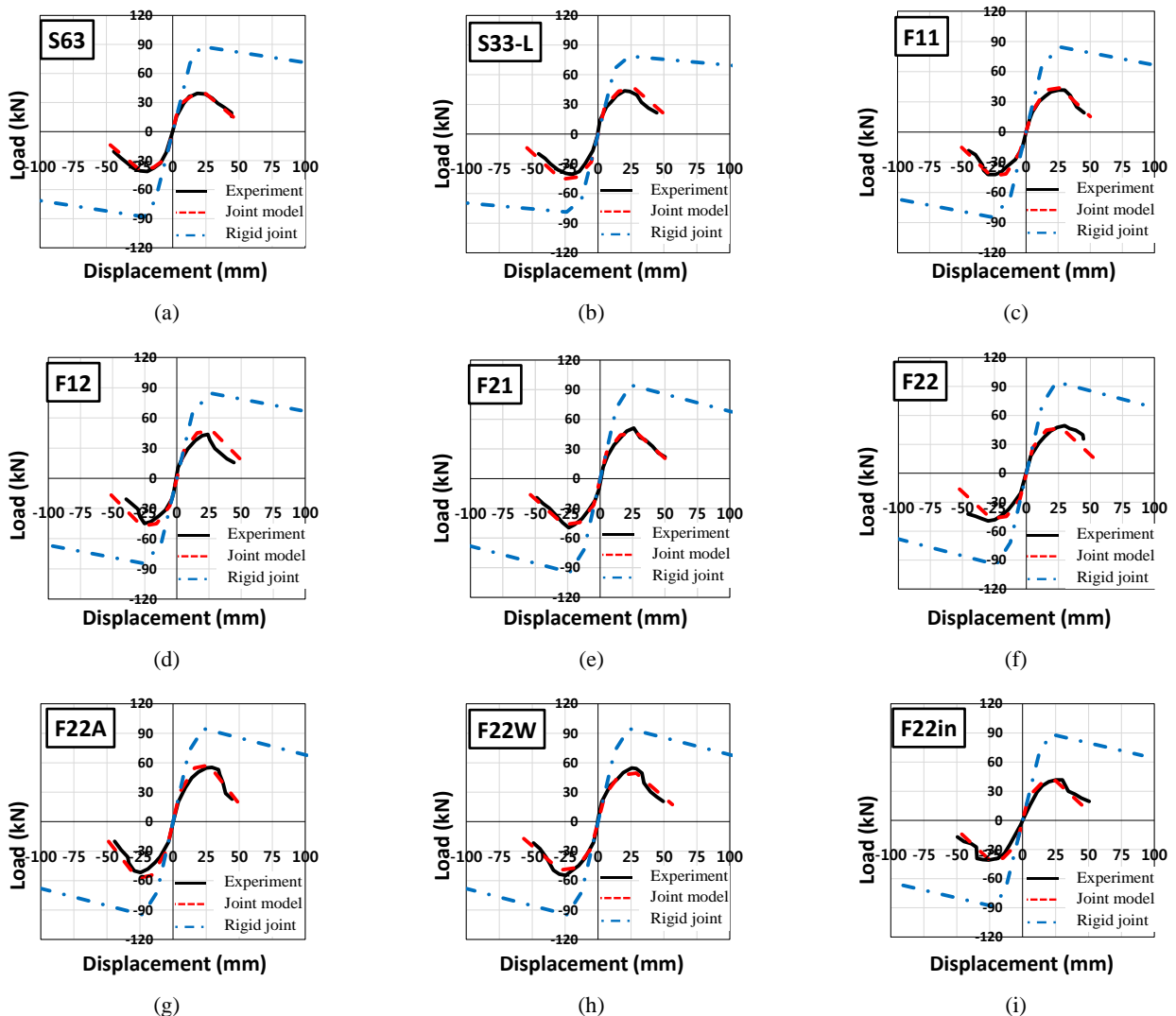


Fig. 16 Validation of the proposed numerical model against tests conducted by Antonopoulos and Triantafillou (2003)

## 5. Validation of the proposed model with experiments

This section evaluates the reliability of the proposed analytical model to carry out nonlinear analysis on FRP strengthened joints. The results obtained from nonlinear analyses were compared to experimental results. For each specimen, in order to appropriately assess the dominant role of the joint core in nonlinear analyses, two nonlinear analyses were performed, one taking into account the joint nonlinearities in nonlinear analyses and another assuming the joint core as rigid. To extensively verify the capability of the proposed analytical model, the results of the numerical analyses on as-built and FRP strengthened joints in terms of the maximum principle tensile stress and the horizontal shear strength in the joint core were also compared to experimental results reported by other researchers (Antonopoulos and Triantafillou 2003, Parvin *et al.* 2010, Garcia *et al.* 2013, Eslami and Ronagh 2014). Furthermore, to evaluate the accuracy of the proposed analytical model in the prediction of the shear capacity of FRP strengthened joints, the results obtained from it were compared with those obtained from existing analytical models available in the literature (Antonopoulos and Triantafillou 2002, Bousselham 2010, Akguzel and Pampanin 2012, Del Vecchio *et al.* 2015 and Hadi and Tran 2015) which were developed to calculate the shear capacity of FRP strengthened joints. It should be noted that nonlinear analyses were carried out via the commercial software SAP 2000 (2008).

### 5.1 Prediction of load-displacement response

To evaluate the accuracy of the definition of diagonal axial springs characteristics as well as beam and column plastic hinges for FRP strengthened joints, the response of tests conducted by Antonopoulos and Triantafillou (2003), Parvin *et al.* (2010), Garcia *et al.* (2013), Eslami and Ronagh (2014) in terms of load–displacement relation were predicted by nonlinear analysis based on the proposed model.

Antonopoulos and Triantafillou (2003) tested nine exterior RC joints strengthened by FRP with different configurations. The beam longitudinal bars were anchored as 90°-hooks. All specimens were designed without shear reinforcement in the joint core. Complete detailed of the

tested specimens can be found from Antonopoulos and Triantafillou (2003). Fig. 16 compares the responses obtained from the experiment and the numerical analyses. As can be seen, very good agreement between numerical and experimental results proves that the proposed numerical model can simulate the response of the FRP strengthened joints. It can be concluded that regardless of nonlinearities in the joint core, the nonlinear analysis might estimate by far higher ductility and strength than the ones reported from experiments and failure mechanism also occurred in beam strengthened region.

On the other hand, using proposed model, for all the specimens, the failure modes were predicted as the failure in the joint panel (the concrete diagonal cracking or the failure or debonding of the FRP) which was similar to the failure mode reported by the experiment.

Three exterior RC beam-column joints strengthened by FRP sheets tested by Garcia *et al.* (2013) were modeled here.

Top and bottom of the beam longitudinal bars were anchored with 90°-hooks and adequate embedment length in the joint core, respectively. Since increasing the length of the development of beam bars embedded as straight anchorage, the bond mechanism between concrete and rebars would not merely be the critical parameter. In such cases, it is expected that the bond failure occurs after the diagonal compressive strut could be fully developed. Accordingly, to determine the characteristics of the diagonal axial springs in the joint core, for both loading directions, the principle tensile stress – joint rotation proposed for joints with 90°-hooks was followed. Complete detailed of the tested specimens can be found from Garcia *et al.* (2013). In Fig. 17 the load-displacement curves reported from the experiment were compared with the ones obtained from numerical analyses (to appropriately examine the accurate of the proposed model in the prediction of FRP strengthened joints in terms of strength and ductility, the result of analysis with no joint model was not reported). Although the test results for specimen of JA2RF seem to be virtually non-conservative, for other specimens, the analyses led to slightly conservative results. Overall, a closer look at the data reveals that the developed model, to simulate the effect of FRP material on inelastic behaviour of the beam-column joints, is capable of properly estimating initial stiffness and shape of response envelope.

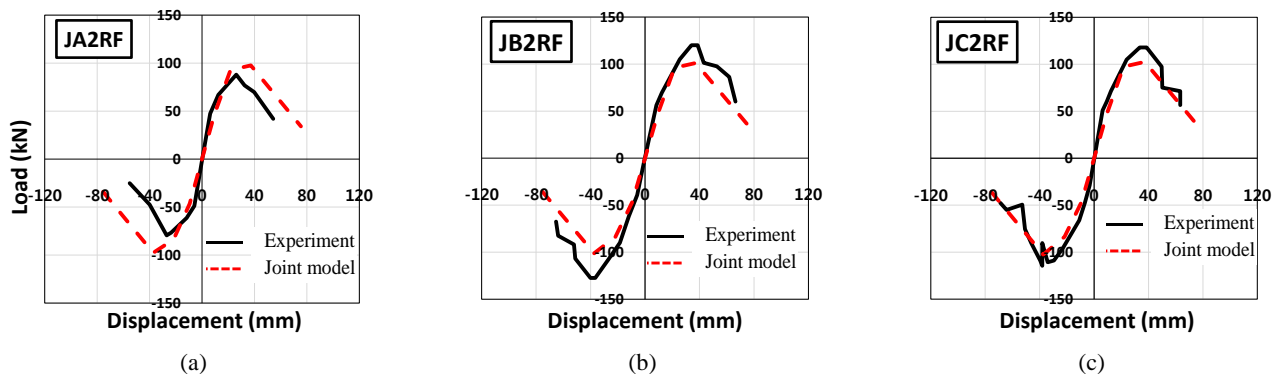


Fig. 17 Validation of the proposed numerical model against tests conducted by Garcia *et al.* (2013)

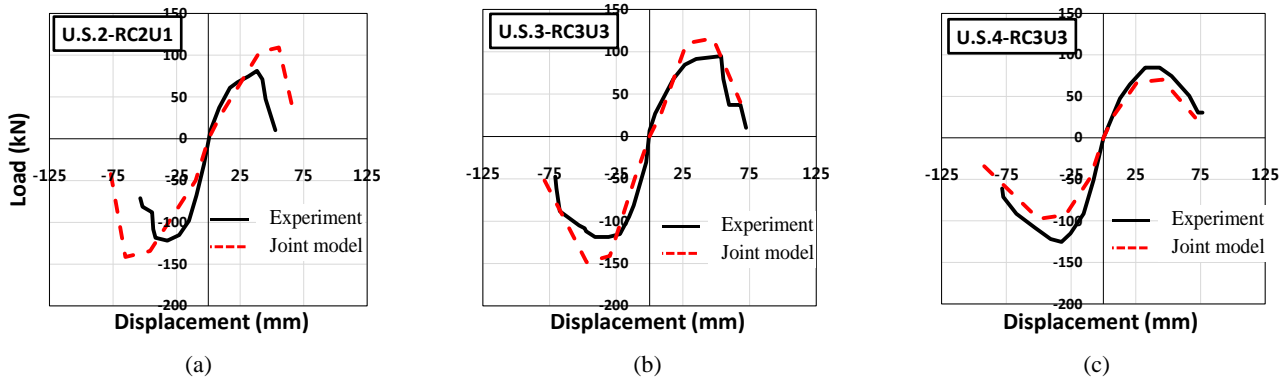


Fig. 18 Validation of the proposed numerical model against tests conducted by Parvin *et al.* (2010)

Parvin *et al.* (2010) conducted an experimental study on FRP strengthened joints without stirrup in the joint core subjected to cyclic loading applied at the tip of the column. All of the three tested specimens are identical in details and dimensions. Top and bottom of the beam longitudinal bars were anchored as 90°-hooks and embedded as straight anchorage the joint core, respectively. Complete detailed of the tested specimens can be found from Parvin *et al.* (2010). The load - displacement curves at the column tip of the strengthened joints reported from the experiment were compared with the numerical results as shown in Fig. 18. Again, the results indicated that taking into account the joint core effect, the proposed numerical model would be able to simulate the response of the joints strengthened by FRP materials with reasonably good agreement. In specimen of U.S.2-RC2U1, the joint response in terms of strength ductility was predicted slightly higher than the one reported by the experiment. Furthermore, in specimens of U.S.3-RC3U3 and U.S.4-RC3U3, the joint strength observed by the experiment, was virtually overestimated and underestimated, respectively, while ductility was approximately estimated with reasonable accurate.

In order to examine the capability of FRP sheets to relocate inelastic hinges at a controlled distance from the adjacent of the joint core, Eslami and Ronagh (2014) conducted a test on FRP strengthened beam-column joint with shear reinforcements in the joint core. Complete detailed of the tested specimens can be found from Eslami and Ronagh (2014). It should be noted that the procedure

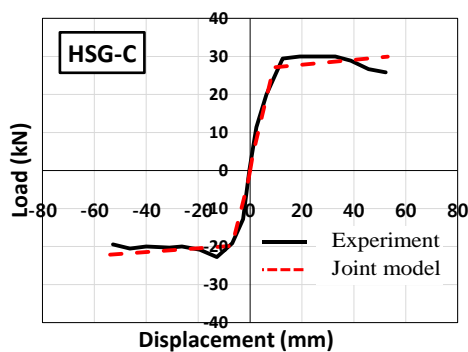


Fig. 19 Validation of the proposed numerical model against tests conducted by Eslami and Ronagh (2014)

proposed by Shayanfar *et al.* (2016) was adopted to take into account the effect of shear reinforcements in the joint core on principle tensile stress – joint rotation relation. Fig. 19 compared load-displacement curves resulted and reported from numerical analysis and the experiment. As can be seen, the numerical model would accurately predict the response of the FRP strengthened beam-column joint due to appropriately estimating inelastic characteristics of members. Moreover, similar to the experiment, the failure mode obtained from numerical analysis was determined as beam flexural failure at the end of the beam FRP sheets. It confirms the reliability of the numerical model in simulating FRP strengthened joints with failure mode as beam failure at the end of the strengthened region.

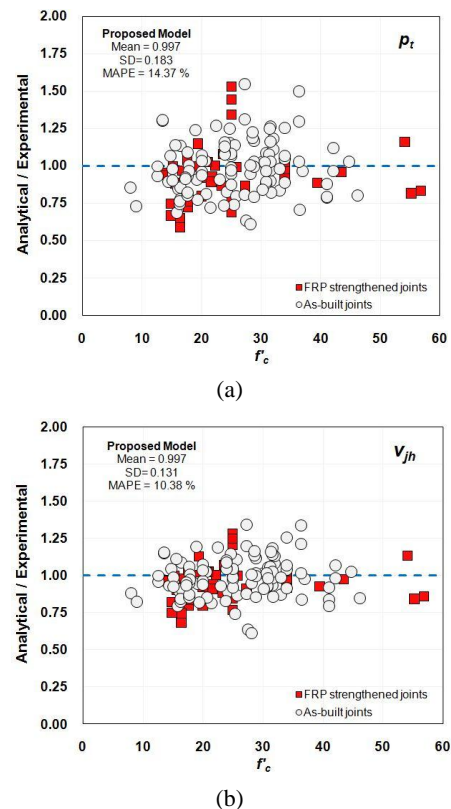


Fig. 20 Prediction of maximum principle tensile stress: (a) and shear capacity; (b) for as-built and FRP strengthened joints by the proposed model

Table 2 Comparing between proposed and existing models to predict the shear capacity of FRP strengthened joints which test by Antonopoulos and Triantafillou (2003) ( $v_{jh}/v_{jh}^{EXP}$ )

Title	Antonopoulos and Triantafillou (2002)	Bousselham (2010)	Akguzel and Pampanin (2012)	Del Vecchio <i>et al.</i> (2015)	Hadi and Tran (2015)	Proposed model
<b>F11</b>	0.97	0.71	0.97	0.96	0.97	1.04
<b>F22</b>	1.23	0.78	1.06	1.01	0.93	0.92
<b>F21</b>	1.05	0.76	0.96	0.95	0.90	0.93
<b>F12</b>	1.23	0.74	1.10	1.09	1.05	1.03
<b>F22W</b>	1.12	0.71	0.97	1.19	0.86	0.83
<b>GL</b>	0.91	0.66	0.85	0.88	0.88	1.01
<b>F22A</b>	- <sup>a</sup>	0.83	1.03	1.06	1.01	0.88
<b>F22in</b>	-	0.87	1.12	0.98	1.00	0.96
<b>S33L</b>	-	0.87	0.98	1.03	0.97	1.01
<b>S63</b>	-	1.01	1.16	1.07	1.09	0.98
<b>S-F22</b>	-	0.81	-	1.01	1.05	1.07
<b>T-F33</b>	-	0.79	-	1.06	-	1.02
<b>T-F22S2</b>	-	0.99	-	0.99	-	1.04
<b>Mean</b>	<b>1.085</b>	<b>0.810</b>	<b>1.020</b>	<b>1.022</b>	<b>0.965</b>	<b>0.991</b>
<b>SD</b>	<b>0.112</b>	<b>0.071</b>	<b>0.086</b>	<b>0.074</b>	<b>0.069</b>	<b>0.066</b>
<b>MAPE</b>	<b>12.5%</b>	<b>19.2%</b>	<b>7.4%</b>	<b>5.9%</b>	<b>6.3%</b>	<b>5.5%</b>

<sup>a</sup> Denotes the results of FRP strengthened joints that were not reported by researchers (not available)

### 5.2 Prediction of maximum principle tensile stress and shear strength

In this section, the accuracy of the proposed model in predicting the principle tensile stress and shear strength in the joint core will be examined. In order to verify, for as-built and strengthened joints, the proposed principle tensile stress and the corresponding horizontal shear strength were applied to the tested specimens (Appendix B and C) as

shown in Fig. 20. As can be seen, using the proposed model, the mean of the ratio of the principle tensile stress and horizontal shear strength obtained-to-experimental was calculated equal to 0.997 with SD 0.183 and 0.131 along with a MAPE, 14.37% and 10.38%, respectively. Taking into account these values, it can be concluded that the model proposed in current paper can provide the uniform prediction of the as-built and FRP strengthened joints capacity with reasonable precision. Therefore, it does not

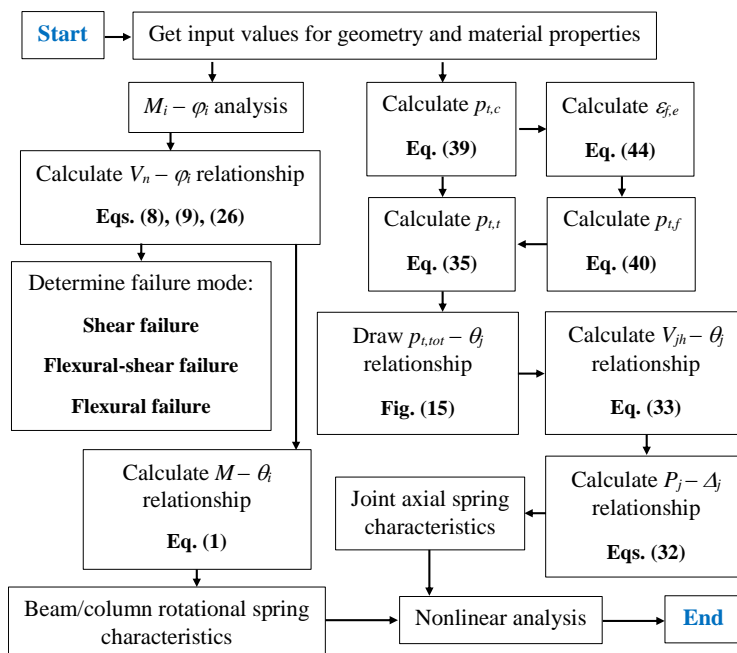


Fig. 21 A flowchart for obtaining the characteristics of axial and rotational springs

seem unreasonable to express that the existing models predict the response of the as-built joints with a relatively high level of dispersion. In order to evaluate the accuracy and reliability of the proposed analytical procedure in predicting the shear capacity of FRP strengthened joints, Table 2 provide a comparison between results obtained from proposed analytical procedure and existing models (Antonopoulos and Triantafillou 2002, Bousselham 2010, Akguzel and Pampanin 2012, Del Vecchio *et al.* 2015 and Hadi and Tran 2015) and reported from the experiment conducted by Antonopoulos and Triantafillou (2003). As can be seen in Table 2, with respected to the values of mean, MAPE and SD, the best estimates in terms of  $v_{jh}/v_{jh}^{exp}$  was provided by using proposed analytical procedure that it confirms its reliability for simulating FRP strengthened joints.

In Fig. 21, a flowchart was provided for obtaining spring characteristics of  $P_j - \Delta_j$  of the joint core as well as  $M - \theta_j$  of beam and columns.

As can be seen, once beam/column moment-curvature relation was determined, flexural and shear capacities can be computed by the simple procedure to control shear mechanism. On the other hand, the diagonal axial spring characteristics can be easily obtained by converting the proposed principle tensile stress – joint rotation into axial load – axial displacement. According to the capability of the developed beam – column joint in terms of the accuracy and being practical, it seems to be appropriate not only to simulate as-built and FRP strengthened joints, but also in engineering practice as a practical procedure.

## 6. Conclusions

In current paper, taking into account the effects of FRP sheets on inelastic behaviour of the joint core, a new procedure was proposed for modelling FRP strengthened beam-column joints in a numerical analysis. In order to compute the inelastic characteristics of the joint core, for as-built and FRP strengthened beam-column joints with various anchorage of beam bars, principal tensile stress-joint rotation relations have been proposed according to experimental results and a combination of a mechanically-based model. On the other hand, the effect of shear mechanism in as built and FRP strengthened beams/columns was considered developing practical formulations.

To assess the reliability of the proposed numerical model, results reported from the experimental studies available in the literature were compared to the ones obtained from nonlinear analysis. The results proved that the proposed joint model can predict the response of FRP strengthened beam-column joints with reasonable accuracy.

Based on this study, not taking into account nonlinearities in the core of FRP strengthened joints might lead to unsafe and non-conservative prediction in terms of strength and ductility. Ultimately, the proposed numerical model could present a practical but accurate procedure for engineers to model the response of FRP strengthened joints taking into account inelastic behaviour of the joint core in nonlinear analyses.

## References

- ACI 440.2R-02 (2002), Guide for the design and construction of externally bonded FRP systems for strengthening concrete structures, Committee 440 Report; American Concrete Institute, Detroit, MI, USA.
- Adhikary, B.B., Mutsuyoshi, H. and Ashraf, M. (2004), “Shear strengthening of reinforced concrete beams using fiber-reinforced polymer sheets with bonded anchorage”, *Struct. J.*, **101**(5), 660-668.
- Akbarzadeh, B.H. and Shayanfar, J. (2015), “Seismic performance of RC frames joints retrofitted by CFRP composites”, *Proceedings of the 2th International and the 6th National Conference on Earthquake & Structures*, Kerman, Iran, October.
- Akbarzadeh, B.H., Shayanfar, J. and Seyedpour, S.M. (2015), “An artificial neural network (ANN) model for predicting the moment-rotation of exterior RC beam–column joints strengthened by CFRP composites”, *Proceedings of the 2th International and the 6th National Conference on Earthquake & Structures*, Kerman, Iran, October.
- Akbarzadeh, B.H., Abdollahtabar, M. and Shayanfar, J. (2016), “Predicting the Ductility of RC Beams Using Nonlinear Regression and ANN”, *Iran. J. Sci. Technol. Transact. Civil Eng.*, **40**(4), 297-310.
- Akguzel, U. (2011), “Seismic performance of FRP retrofitted exterior RC beam-column joints under varying axial and bidirectional loading”, Ph.D. Dissertation; University of Canterbury, Christchurch, SI, USA.
- Akguzel, U. and Pampanin, S. (2010), “Effects of variation of axial load and bi-directional loading on seismic performance of GFRP retrofitted reinforced concrete exterior beam-column joints”, *J. Compos. Constr.*, **14**(1), 94-104.
- Akguzel, U. and Pampanin, S. (2012), “Assessment and design procedure for the seismic retrofit of reinforced concrete beam–column joints using FRP composite materials”, *J. Compos. Constr.*, **16**, 21-34.
- Allington, C.J. (2003), “Seismic performance of moment resisting frame members produced from lightweight aggregate concrete”, Ph.D. Dissertation; University of Canterbury, Christchurch, SI, USA.
- Al-Salloum, Y.A. and Almusallam, T.H. (2007), “Seismic response of interior beam-column joints upgraded with FRP sheets. II: Analysis and parametric study”, *J. Compos. Constr.*, **11**(6), 575-590.
- Antonopoulos, C.P. and Triantafillou, T.C. (2002), “Analysis of FRP strengthened beam-column joints”, *J. Compos. Constr.*, **6**(1), 41-51.
- Antonopoulos, C.P. and Triantafillou, T.C. (2003), “Experimental investigation of FRP strengthened RC beam column joints”, *J. Compos. Constr.*, **7**, 39-49.
- Biddah, A., and Ghobarah, A. (1999), “Modelling of shear deformation and bond slip in reinforced concrete joints”, *Struct. Eng. Mech., Int. J.*, **7**(4), 413-432.
- Bousselham, A. (2010), “State of research on seismic retrofit of RC beam–column joints with externally bonded FRP”, *J. Compos. Constr.*, **14**, 49-61.
- Calvi, G.M., Magenes, G. and Pampanin, S. (2002), “Relevance of beam–column joint damage and collapse in RC frame assessment”, *J. Earthq. Eng.*, **6**, 75-100.
- Campione, G., Cavaleri, L. and Papia, M. (2015), “Flexural response of external R.C. beam–column joints externally strengthened with steel cages”, *Eng. Struct.*, **104**, 51-64.
- Chalioris, C.E., Favvata, M. and Karayannis, C.G. (2008), “Reinforced concrete beam–column joints with crossed inclined bars under cyclic deformations”, *J. Earthq. Eng. Struct. Dyn.*, **37**, 881-897.
- Chen, W.F. (1982), *Plasticity in Reinforced Concrete*, McGraw-

- Hill, New York, NY, USA, pp. 204-205.
- Clyde, C., Pantelides, C.P. and Reaveley, L.D. (2000), "Performance-based evaluation of exterior reinforced concrete building joints for seismic excitation", Report PEER 2000/05; Pacific Earthquake Engineering Research Center.
- Computer and Structures Inc. (SAP2000) (2008), Analysis References, Berkeley, CA, USA.
- Dalalbashi, A., Eslami, A. and Ronagh, H.R. (2013), "Numerical investigation on the hysteretic behavior of RC joints retrofitted with different CFRP configurations", *J. Compos. Constr.*, **17**, 371-382.
- De Risi, M.T. and Verderame, G.M. (2017), "Experimental assessment and numerical modelling of exterior non-conforming beam-column joints with plain bars", *Eng. Struct.*, **150**, 115-134.
- De Risi, M.T., Ricci, P., Verderame, G.M. and Manfredi, G. (2016), "Experimental assessment of unreinforced exterior beam-column joints with deformed bars", *Eng. Struct.*, **112**, 215-232.
- De Risi, M.T., Ricci, P. and Verderame, G.M. (2017), "Modelling exterior unreinforced beam-column joints in seismic analysis of non-ductile RC frames", *Earthq. Eng. Struct. Dyn.*, **46**(6), 899-923.
- Del Zoppo, M., Di Ludovico, M., Balsamo, A., Prota, A. and Manfredi, G. (2017), "FRP for seismic strengthening of shear controlled RC columns: Experience from earthquakes and experimental analysis", *Compos. Part B: Eng.*, **129**, 47-57.
- Del Vecchio, C., Di Ludovico, M., Balsamo, A., Prota, A., Manfredi, G. and Dolce, M. (2014), "Experimental investigation of exterior RC beam-column joints retrofitted with FRP systems", *J. Compos. Constr.*, **18**, 1-13.
- Del Vecchio C., Di Ludovico, M., Prota, A. and Manfredi, G. (2015), "Analytical model and design approach for FRP strengthening of non-conforming RC corner beam-column joints", *Eng. Struct.*, **87**, 8-20.
- Del Vecchio, C., Di Ludovico, M., Prota, A. and Manfredi, G. (2016), "Modelling beam-column joints and FRP strengthening in the seismic performance assessment of RC existing frames", *Compos. Struct.*, **142**, 107-116.
- Del Vecchio, C., Gentile, E.R. and Pampanin, S. (2017), "The simplified lateral mechanism analysis (SLaMa) for the seismic performance assessment of a case study building damaged in the 2011 Christchurch earthquake", Research Report 2016-02; Civil & Natural Resources Engineering.
- Di Ludovico, M., Balsamo, A., Prota, A., Verderame, G.M., Dolce, M. and Manfredi, G. (2012), "Preliminary results of an experimental investigation on RC beam-column joints", CICE Rome: International Institute for FRP in Construction, p. 1-9.
- El-Amoury, T. (2003), "Seismic rehabilitation of concrete frame beam-column joints", Ph.D. Dissertation; McMaster University, ON, Canada.
- El-Amoury, T. and Ghobarah, A. (2002), "Seismic rehabilitation of beam-column joint using GFRP sheets", *Eng. Struct.*, **24**, 1397-1407.
- Elmorsi, M., Kianoush, M.R. and Tso, W.K. (2000), "Modeling bond-slip deformations in reinforced concrete beam-column joints", *Can. J. Civ. Eng.*, **273**, 490-505.
- Elwood, K. (2002), "Shake table tests and analytical studies on the gravity load collapse of reinforced concrete frames", Ph.D. Dissertation; University of California, Berkeley, CA, USA.
- Eslami, A. and Ronagh, H.R. (2014), "Experimental investigation of an appropriate anchorage system for flange-bonded carbon fiber reinforced polymers in retrofitted RC beam-column joints", *J. Compos. Constr.*, **18**(4), 04013056.
- Eslami, A. and Ronagh, H. (2015), "Numerical Investigation on the Seismic Retrofitting of RC Beam-Column Connections Using Flange-Bonded CFRP Composites", *J. Compos. Constr.*, **20**(1), 04015032.
- Eslami, A., Dalalbashi, A. and Ronagh, H.R. (2013), "On the effect of plastic hinge relocation in RC buildings using CFRP", *Compos. Part B: Eng.*, **52**, 350-361.
- Fakharifar, M., Sharbatdar, M.K., Lin Z., Dalvand, A., Sivandi-Pour, A. and Chen, G. (2014), "Seismic performance and global ductility of RC frames rehabilitated with retrofitted joints by CFRP laminates", *Earthq. Eng. Vib.*, **13**(1), 59-73.
- Favvata, M.J., Izzuddin, B.A. and Karayannis, C.G. (2008), "Modelling exterior beam-column joints for seismic analysis of RC frame structures", *Earthq. Eng. Struct. Dyn.*, **37**(13), 1527-1548.
- Galal, K., Arafa, A. and Ghobarah, A. (2005), "Retrofit of RC square short columns", *Eng. Struct.*, **27**(5), 801-813.
- Garcia, R., Jemaa, Y., Helal, Y., Maurizio, G. and Pilakoutas, K. (2013), "Seismic strengthening of severely damaged beam-column RC joints using CFRP", *J. Compos. Constr.*, **18**(2), 04013048.
- Genesio, G. (2012), "Seismic assessment of RC exterior beam-column joints and retrofit with haunches using post-installed anchors", Ph.D. Dissertation; University of Stuttgart, Stuttgart, Germany.
- George, I., Kalogeropoulos, G., Tsonos, A.G., Konstandinidis, D. and Tsetines, S. (2016), "Pre-earthquake and post-earthquake retrofitting of poorly detailed exterior RC beam-to-column joints", *Eng. Struct.*, **109**, 1-15.
- Gergely, B.J., Pantelides, C.P. and Reaveley, L.D. (2000), "Shear strengthening RCT-joints using CFRP composites", *J. Compos. Constr.*, **4**, 56-64.
- Ghobarah, A. and El-Amoury, T. (2005), "Seismic rehabilitation of deficient exterior concrete frame joints", *J. Compos. Constr.*, **9**, 408-416.
- Ghobarah, A. and Galal, K. (2004), "Seismic rehabilitation of short rectangular RC columns", *J. Earthq. Eng.*, **8**, 45-68.
- Ghobarah, A. and Said, A. (2001), "Seismic rehabilitation of beam-column joints using FRP laminates", *J. Earthq. Eng.*, **5**(1), 113-129.
- Ghobarah, A. and Said, A. (2002), "Shear strengthening of beam-column joints", *Eng. Struct.*, **24**, 881-888.
- Ha, G.J., Cho, C.G., Kang, H.W. and Feo, L. (2013), "Seismic improvement of RC beam-column joints using hexagonal CFRP bars combined with CFRP sheets", *Compos. Struct.*, **95**, 464-470.
- Hadi, M.N.S. and Tran, T.M. (2015), "Seismic rehabilitation of reinforced concrete beam-column joints by bonding with concrete covers and wrapping with FRP composites", *Mater. Struct.*, **49**, 1-19.
- Hadi, M.N. and Tran, T.M. (2016), "Seismic rehabilitation of reinforced concrete beam-column joints by bonding with concrete covers and wrapping with FRP composites", *Mater. Struct.*, **49**(1-2), 467-485.
- Hadigheh, S.A., Mahini, S.S. and Maheri, M.R. (2014), "Seismic behavior of FRP-retrofitted reinforced concrete frames", *J. Earthq. Eng.*, **18**(8), 1171-1197.
- Hassan, W.M. (2011), "Analytical and experimental assessment of seismic vulnerability of beam-column joints without transverse reinforcement in concrete buildings", Ph.D. Dissertation; University of California, Berkeley, CA, USA.
- Helal, Y. (2012), "Seismic strengthening of deficient exterior RC beam-column sub-assemblages using posttensioned metal strips", Ph.D. Dissertation; Department of Civil & Structural Engineering, University of Sheffield, England.
- Hognestad, E. (1951), "A Study of Combined Bending and Axial Load in Reinforced Concrete Members", Bulletin 399, Engineering Experimental Station, University of Illinois, IL, USA.
- Ho, J.C.M. and Pam, H.J. (2003), "Inelastic design of low-axially

- loaded high-strength reinforced concrete columns”, *Eng. Struct.*, **25**(8), 1083-1096.
- Holzenkämpfer, P. (1994), “Ingenieurmodelle des verbundes geklebterbewehrung für betonbauteile”, Ph.D. Dissertation; TU Braunschweig. [In German]
- Kam, W.Y. (2010), “Selective Weakening and Post-tensioning for the Seismic Retrofit of Non-Ductile RC Frames”, Ph.D. Dissertation; University of Canterbury, Christchurch, New Zealand.
- Karayannis, C.G. and Sirkelis, G. (2008), “Strengthening and rehabilitation of RC beam-column joints using carbon-FRP jacketing and epoxy resin injection”, *Earthq. Eng. Struct. Dyn.*, **37**(5), 769-790.
- Karayannis, C.G., Chalioris, C.E. and Sideris, K.K. (1998), “Effectiveness of RC beam-column connection repair using epoxy resin injections”, *J. Earthq. Eng.*, **2**(2), 217-240.
- Karayannis, C.G., Chalioris, C.E. and Sirkelis, G.M. (2008), “Local retrofit of external RC beam column joints using thin RC jackets: An experimental study”, *J. Earthq. Eng. Struct. Dyn.*, **37**(5), 727-746.
- Kaya, O., Yalcin, C., Parvin, A. and Altay, S. (2008), “Repairing of shear-damaged RC joint panel zone using chemical epoxy injection methodology”, *Proceedings of 14th World Conference on Earthquake Engineering*, Beijing, China.
- Kheyroddin, A., Khalili, A., Emami, E. and Sharbatdar, M.K. (2016), “An innovative experimental method to upgrade performance of external weak RC joints using fused steel prop plus sheets”, *Steel Compos. Struct., Int. J.*, **21**(2), 443-460.
- Kim, C.G., Eom, T.S., Park, H.G. and Kim, T.W. (2016), “Seismic Performance of Lightly Reinforced Concrete Beam-Column Connections for Low-Rise Buildings”, *J. Architect. Inst. Korea Struct. Constr.*, **32**(3), 19-30.
- Kwan, A.K.H., Dong, C.X. and Ho, J.C.M. (2015), “Axial and lateral stress-strain model for FRP confined concrete”, *Eng. Struct.*, **99**, 285-295.
- Laterza, M., D’Amato, M. and Gigliotti, R. (2017), “Modeling of gravity-designed RC sub-assemblages subjected to lateral loads”, *Eng. Struct.*, **130**, 242-260.
- Lee, J.H. and Shin, S.J. (2010), “Shear Strength Prediction of FRP RC Baem without Shear Reinforcements”, *J. Korea Concrete Inst.*, **22**(3), 313-324.
- Le-Trung, K., Lee, K., Lee, J., Lee, D.H. and Woo, S. (2010), “Experimental study of RC beam-column joints strengthened using CFRP composites”, *Compos. Part B: Eng.*, **41**(1), 76-85.
- Liu, C. (2006), “Seismic behaviour of beam-column joint subassemblies reinforced with steel fibers”, Master Thesis; University of Canterbury, Christchurch, New Zealand.
- Lowes, L.N. and Altoontash, A. (2003), “Modeling reinforced-concrete beam-column joints subjected to cyclic loading”, *J. Struct. Eng.*, 1686-1697.
- Lynn, A.C. (2001), “Seismic evaluation of existing reinforced concrete building columns”, Ph.D. Dissertation; University of California, Berkeley, CA, USA.
- Mahini, S.S. and Ronagh, H.R. (2011), “Web-bonded FRPs for relocation of plastic hinges away from the column face in exterior RC joints”, *Compos. Struct.*, **93**, 2460-2472.
- Mander, J.B., Priestley, M.J.N. and Park, R. (1988), “Theoretical stress-strain behavior of confined concrete”, *J. Struct. Eng.*, **114**(8), 1804-1826.
- Manfredi, G. and Realfonzo, R. (2001), “Modellazione del comportamento di elementi presso-inflessi in c.a. confinati con tessuti in materiale composito”, Tech. Rep., 10 Convegno Nazionale “L’ingegneria Sismica in Italia”, Potenza-Matera, Italy.
- Melo, J., Varum, H., Rossetto, T. and Costa, A. (2012), “Cyclic response of RC beam-column joints reinforced with plain bars: an experimental testing campaign”, *Proceedings of 15th World Conference on Earthquake Engineering*, Lisbon, Portugal.
- Mitra, N. and Lowes, L. (2007), “Evaluation, calibration, and verification of a reinforced concrete beam-column joint model”, *J. Struct. Eng.*, **133**(1), 105-120.
- Moretti, M. and Tassios, T.P. (2007), “Behaviour of short columns subjected to cyclic shear displacements: Experimental results”, *Eng. Struct.*, **29**(8), 2018-2029.
- Murty, C.V.R., Rai, D., Bajpai, K.K. and Jain, S.K. (2003), “Effectiveness of reinforcement details in exterior reinforced concrete beam-column joints for earthquake resistance”, *ACI Struct. J.*, **100**(2), 149-156.
- Najafgholipour, M.A., Dehghan, S.M., Dooshabi, A. and Niroomandi, A. (2017), “Finite element analysis of reinforced concrete beam-column connections with governing joint shear failure mode”, *Latin Am. J. Solids Struct.*, **14**(7), 1200-1225.
- Neubauer, U. and Rostasy, F.S. (1997), “Design aspects of concrete structures strengthened with externally bonded CFRP-plates”, *Proceedings of the 7th International conference on Structural Faults and Repair*, London, England, July.
- Niroomandi, A., Maheri, A., Maheri, M.R. and Mahini, S.S. (2010), “Seismic performance of ordinary RC frames retrofitted at joints by FRP sheets”, *Eng. Struct.*, **32**, 2326-2336.
- Niroomandi, A., Najafgholipour, M.A. and Ronagh, H.R. (2014), “Numerical investigation of the affecting parameters on the shear failure of nonductile RC exterior joints”, *Eng. Failure Anal.*, **46**, 62-75.
- Niroomandi, A., Pampanin, S., Dhakal, R. and Soleymani Ashtiani, M. (2015), “Comparison of alternative assessment procedures to predict seismic performance of RC columns”, In: *Proceedings of Tenth Pacific Conference on Earthquake Engineering*, Sydney, Australia.
- Omidi, B. and Behnamfar, F. (2015), “A numerical model for simulation of RC beam-column connections”, *Eng. Struct.*, **88**, 51-73.
- O’Reilly, G.J. and Sullivan, T.J. (2017), “Modeling techniques for the seismic assessment of the existing Italian RC frame structures”, *J. Earthq. Eng.*, 1-35.
- Pantazopoulou, S. and Bonacci, J. (1992), “Consideration of questions about beam-column joints”, *ACI Struct. J.*, **89**(1), 27-36.
- Parvin, A. and Granata, P. (2000), “Investigation on the effects of fiber composites at concrete joints”, *Compos. Part. B: Eng.*, **31**, 499-509.
- Parvin, A. and Wu, S. (2008), “Ply angle effect on fiber composite wrapped reinforced concrete beam-column connections under combined axial and cyclic loads”, *Compos. Struct.*, **82**(4), 532-538.
- Parvin, A., Altay, S., Yalcin, C. and Kaya, O. (2010), “CFRP Rehabilitation of concrete frame joints with inadequate shear and anchorage details”, *J. Compos. Constr.*, **14**(1), 72-82.
- Pampanin, S., Calvi, G.M. and Moratti, M. (2002), “Seismic behavior of RC beam-column joints designed for gravity only”, *Proceedings of the 12th European Conference on Earthquake Engineering (ECEE)*, London, UK.
- Pampanin, S., Magenes, G. and Carr, A. (2003), “Modelling of shear hinge mechanism in poorly detailed RC beam-column joints”, *Fib Symposium on Concrete Structures in Seismic Regions*, Athens, Greece, May.
- Pampanin, S., Christopoulos, C. and Chen, T.H. (2006), “Development and validation of a metallic haunch seismic retrofit solution for existing under-designed RC frame buildings”, *Earthq. Eng. Struct. D.*, **35**, 1739-1766.
- Pampanin, S., Bolognini, D. and Pavese, A. (2007), “Performance-based seismic retrofit strategy for existing RC frame systems using FRP composites”, *J. Compos. Constr.*, **11**(2), 211-226.
- Pantelides, C.P., Hansen, J., Nadauld, J. and Reaveley, L.D. (2002), “Assessment of reinforced concrete building exterior

- joints with substandard details”, Report no. PEER 2002/18; Pacific Earthquake Engineering Research Center.
- Park, S. and Mosalam, K.M. (2012), “Parameters for shear strength prediction of exterior beam-column joints without transverse reinforcement”, *Eng. Struct.*, **36**, 198-209.
- Park, R., Priestley, M.J.N. and Gill, W.D. (1982), “Ductility of square-confined concrete columns”, *J. Struct. Eng.*, **108**, 929-950.
- Park, H., Choi, K. and Wight, J.K. (2006), “Strain-based shear strength model for slender beams without web reinforcement”, *ACI Struct. J.*, **103**(6), 783-793.
- Park, H., Yu, E. and Choi, K. (2012), “Shear-strength degradation model for RC columns subjected to cyclic loading”, *Eng. Struct.*, **34**, 187-197.
- Paulay, T. and Priestley, M.J.N. (1992), *Seismic Design of Reinforced Concrete and Masonry Buildings*, John Wiley Publications, New York, NY, USA.
- Priestley, M.J.N. (1997), “Displacement based seismic assessment of reinforced concrete buildings”, *J. Earthq. Eng.*, **1**(1), 157-192.
- Priestley, M.J.N., Verma, R. and Xiao, Y. (1994), “Seismic shear strength of reinforced concrete columns”, *J. Struct. Eng.*, **120**(8), 2310-2329.
- Priestley, M.J.N., Seible, F. and Calvi, G.M. (1996), *Seismic Design and Retrofit of Bridge Structures*, John Wiley and Sons, New York, NY, USA.
- Realfonzo, R., Napoli, A. and Pinilla, J.G.R. (2014), “Cyclic behavior of RC beam-column joints strengthened with FRP systems”, *Constr. Build. Mater.*, **54**, 282-297.
- Ricci, P., De Risi, M.T., Verderame, G.M. and Manfredi, G. (2016), “Experimental tests of unreinforced exterior beam-column joints with plain bars”, *Eng. Struct.*, **118**, 178-194.
- Ronagh, H.R. and Eslami, A. (2013), “Flexural retrofitting of RC buildings using GFRP/CFRP – A comparative study”, *Compos. Part B: Eng.*, **46**, 188-196.
- Sezen, H. (2002), “Seismic behavior and modeling of reinforced concrete building columns”, Ph.D. Dissertation; University of California, Berkeley, CA, USA.
- Sezen, H. and Moehle, J.P. (2004), “Shear strength model for lightly reinforced concrete columns”, *J. Struct. Eng.*, **130**(11), 1692-1703.
- Shafaei, J., Zareian, M.S., Hosseini, A. and Marefat, M.S. (2014), “Effects of joint flexibility on lateral response of reinforced concrete frames”, *Eng. Struct.*, **81**, 412-431.
- Sharma, A. (2013), “Seismic behavior and retrofitting of RC frame structures with emphasis on beam-column joints – experiments and numerical modeling”, Ph.D. Dissertation; University of Stuttgart, Stuttgart, Germany.
- Sharma, A., Eligehausen, R. and Reddy, G.R. (2011), “A new model to simulate joint shear behavior of poorly detailed beam-column connections in RC structures under seismic loads, part I: exterior joints”, *Eng. Struct.*, **33**, 1034-1051.
- Shayanfar, J. and Akbarzadeh, B.H. (2016a), “Numerical model to simulate shear behaviour of RC joints and columns”, *Comput. Concrete*, **18**(4), 877-901.
- Shayanfar, J. and Akbarzadeh, B.H. (2016b), “Nonlinear analysis of RC frames considering shear behaviour of members under varying axial load”, *Bull. Earthq. Eng.*, 1-24.
- Shayanfar, J., Akbarzadeh B.H. and Niroomandi, A. (2016), “A proposed model for predicting nonlinear behavior of RC joints under seismic loads”, *Mater. Des.*, **95**, 563-579.
- Shin, M. and LaFave, J.M. (2004), “Testing and modelling for cyclic joint shear deformations in RC beam-column connections”, *Proceedings of the 13th world conference on earthquake engineering*, London, England, August.
- Shrestha, R., Smith, S.T. and Samali, B. (2009), “Strengthening RC beam-column connections with FRP strips”, *Proceedings of the Institution of Civil Engineers – Structures and Buildings* **162**(5), 323-334.
- Sung, Y.C., Liu, K.Y., Su, C.K., Tsai, I.C. and Chang, K.C. (2005), “A study on pushover analyses of reinforced concrete columns”, *J. Struct. Eng. Mech.*, **21**, 35-52.
- Tasligedik, A.S. (2017), “Capacity estimation of FRP strengthened RC beam-column joints using hierarchy of strength assessment”, *Bull. Earthq. Eng.*, 1-18.
- Tasligedik, A.S., Akguzel, U., Kam, W.Y. and Pampanin, S. (2016), “Strength hierarchy at reinforced concrete beam-column joints and global capacity”, *J. Earthq. Eng.*, 1-34.
- Triantafyllou, T.C. (1998), “Shear strength of reinforced concrete beams using epoxy-bonded FRP composites”, *ACI Struct. J.*, **95**(2), 107-115.
- Truong, G.T., Dinh, N.H., Kim, J.C. and Choi, K.K. (2017), “Seismic performance of exterior RC beam-column joints retrofitted using various retrofit solutions”, *Int. J. Concrete Struct. Mater.*, **11**(3), 415-433.
- Tsonos, A.G. (2001), “Seismic rehabilitation of reinforced concrete joints by the removal and replacement technique”, *Eur. Earthq. Eng.*, **3**, 29-43.
- Tsonos, A.G. (2002a), “Seismic repair of exterior R/C beam-to-column joints using two sided and three-sided jackets”, *Struct. Eng. Mech., Int. J.*, **13**, 17-34.
- Tsonos, A.G. (2002b), “Seismic repair of exterior R/C beam-to-column joints using two sided jackets”, *Struct. Eng. Mech., Int. J.*, **13**(1), 17-34.
- Tsonos, A.G. (2014), “An innovative solution for strengthening old R/C structures and for improving the FRP strengthening method”, *Struct. Monit. Mainten. Int. J.*, **1**(3), 323-338.
- Wang, Y.C. and Restrepo, J.I. (2001), “Investigation of concentrically loaded reinforced concrete columns confined with glass fiber-reinforced polymer jackets”, *ACI Struct. J.*, **98**(3), 377-385.
- Wong, H.F. (2005), “Shear strength and seismic performance of non-seismically designed reinforced concrete beam-column joints”, Ph.D. Dissertation; Hong Kong University of Science and Technology, Kwoloon, Hong Kong.
- Yurdakul, O. and Avsar, O. (2016), “Strengthening of substandard reinforced concrete beam-column joints by external post-tension rods”, *Eng. Struct.*, **107**, 9-22.

CC

## Appendix A

According to Shayanfar *et al.* (2016), to convert  $V_b$  and  $V_c$  into diagonal axial force in the joint core, force equilibrium corresponding to the beam-column joint model was used (Fig. A1). Accordingly, based on the equilibrium in elements 1 and 2, we have

$$M_1 = V_1 \frac{h_c}{2} \quad (\text{A-1})$$

$$M_2 = V_2 \frac{h_c}{2} \quad (\text{A-2})$$

Considering the equilibrium in point "a", we have

$$M_1 - M_2 = M_c \quad (\text{A-3})$$

$$V_1 + V_2 = N_a \quad (\text{A-4})$$

in which

$$M_c = V_c \left( \frac{L_c - h_b}{2} \right) \quad (\text{A-5})$$

where  $N_a$  = the axial load on the column. Substitution of Eqs. (A-1) and (A-2) into Eq. (A-3) and then, rearranging the equation, we get

$$V_1 = \frac{N_a}{2} + \frac{M_c}{h_c} \quad (\text{A-6})$$

$$V_2 = \frac{N_a}{2} - \frac{M_c}{h_c} \quad (\text{A-7})$$

Hence,  $V_5$  and  $V_6$  can be derived via above procedure as

$$V_5 = \frac{M_c}{h_c} - \frac{N_e}{2} \quad (\text{A-8})$$

$$V_6 = -\frac{M_c}{h_c} - \frac{N_e}{2} \quad (\text{A-9})$$

Based on the equilibrium in points "b", "c" and "d" (Fig. A1), we have

$$V_2 = N_3 - P \sin \psi \quad (\text{A-10})$$

$$V_5 = N_4 + P \sin \psi \quad (\text{A-11})$$

$$V_b = N_4 - N_3 \quad (\text{A-12})$$

in which  $\left( \sin \psi = \frac{\alpha}{\sqrt{1+\alpha^2}} \right)$

$$P = \frac{V_5 - V_2 - V_b}{2 \sin \psi} \quad (\text{A-13})$$

Substitution of Eqs. (A-7) and (A-8) into Eq. (A-13) and some simplification, we get

$$P = \frac{V_c (L_c - h_b) - 0.5 V_b h_c}{2 h_b} \sqrt{1 + \alpha^2} \quad (\text{A-14})$$

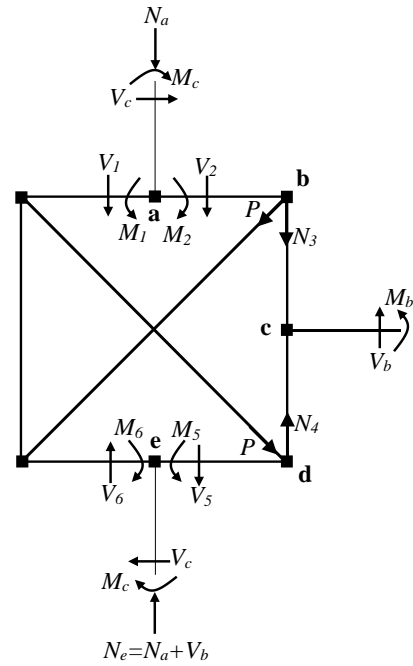


Fig. A1 Force equilibrium corresponding to proposed joint model in Fig. 2 (Shayanfar *et al.* 2016)

## Appendix B

See Tables B1

Table B1 Database of experimental tests on unreinforced exterior beam-column joints

Test ID	Type	$b_b$ (mm)	$h_b$ (mm)	$b_c$ (mm)	$h_c$ (mm)	$f_c^c$ (MPa)	$f_{yb}$ (MPa)	$\rho_b$	$r_N$	$V_b^{exp}$ (kN)	$v_{jh}^{exp}$ (MPa)	$v_c/\sqrt{f_c}$	
Clyde <i>et al.</i> (2000)	2#	A <sup>a</sup>	305	406	305	457	46.2	454	0.021	0.11	290	7.3	0.77
	4#	A	305	406	305	457	41.0	454	0.021	0.24	294	7.4	0.62
	5#	A	305	406	305	457	37.0	454	0.021	0.28	268	6.8	0.55
	6#	A	305	406	305	457	41.1	454	0.021	0.10	276	7.0	0.81
Pantelides <i>et al.</i> (2002)	Unit 1	B <sup>b</sup>	406	406	406	406	33.1	459	0.016	0.10	92	2.6	0.25
	Unit 1	A	406	406	406	406	33.1	459	0.016	0.10	195	5.5	0.72
	Unit 2	B	406	406	406	406	30.2	459	0.016	0.27	190	5.4	0.48
	Unit 2	A	406	406	406	406	34.0	459	0.016	0.10	188	5.3	0.67
	Unit 3	A	406	406	406	406	31.6	459	0.016	0.27	211	6.0	0.55
	Unit 4	A	406	406	406	406	31.7	459	0.016	0.10	194	5.5	0.74
	Unit 5	A	406	406	406	406	30.2	459	0.016	0.27	126	3.6	0.24
Wong (2005)	BS-L	A	260	450	300	300	30.9	520	0.008	0.15	101	3.7	0.36
	BS-L-600	A	260	600	300	300	36.4	520	0.006	0.15	133	3.4	0.25
	BS-LL	A	260	450	300	300	42.1	520	0.008	0.15	128	4.7	0.37
	BS-U	A	260	450	300	300	31.0	520	0.008	0.15	109	4.0	0.41
	BS-L-LS	A	260	450	300	300	31.6	520	0.008	0.15	110	4.1	0.40
	JA-NN03	A	260	400	300	300	44.8	520	0.006	0.03	81	3.4	0.41
	BS-LL	C <sup>c</sup>	260	450	300	300	42.1	520	0.008	0.15	70	2.6	0.14
	BS-OL	C	260	450	300	300	30.9	520	0.008	0.15	64	2.4	0.17
Antonopoulos and Triantafillou (2003)	C1	A	200	300	200	200	15.6	585	0.008	0.07	31	2.2	0.44
	C2	A	200	300	200	200	19.0	585	0.008	0.06	31	2.2	0.40
Garcia <i>et al.</i> (2013)	JA	A	260	400	260	260	32.0	551	0.008	0.07	57	3.0	0.38
	JB	A	260	400	260	260	31.3	551	0.008	0.07	58	3.1	0.39
	JC	A	260	400	260	260	32.0	551	0.008	0.07	55	2.9	0.35
El Amoury (2003)	T-S1	B	250	400	250	400	30.6	477	0.012	0.20	61	2.8	0.19
	T-S1	A	250	400	250	400	30.6	477	0.012	0.20	116	5.2	0.54
Shafaei <i>et al.</i> (2014)	J3	B	220	250	250	250	24.7	460	0.008	0.14	21	2.0	0.17
	J3	A	220	250	250	250	24.7	460	0.011	0.14	41	3.9	0.49
Shrestha <i>et al.</i> (2009)	UCI	A	300	450	300	300	25.6	532	0.013	0.08	83	3.1	0.46
Melo <i>et al.</i> (2014)	TPA-1	A	250	400	250	250	24.2	405	0.003	0.13	28	2.3	0.29
	TPA-2	A	250	400	250	250	25.8	405	0.003	0.12	29	2.4	0.30
	TPB-1	A	250	400	250	250	15.8	405	0.003	0.20	28	2.3	0.35
	TPB-2	A	250	400	250	250	27.3	405	0.003	0.12	30	2.4	0.29
	TP	A	250	400	250	250	21.5	465	0.003	0.15	31	2.6	0.36
	TPC	D <sup>d</sup>	250	400	250	250	23.8	405	0.003	0.13	27	2.2	0.28
De Risi <i>et al.</i> (2016)	1	A	300	500	300	300	28.8	487	0.008	0.10	74	2.8	0.32
	2	A	300	500	300	300	28.8	459	0.003	0.10	58	2.2	0.23
Yurdakul and Avsar (2016)	EJ-R	A	250	500	250	500	8.1	293	0.010	0.10	100	2.0	0.68

Table B1 Continued

Test ID	Type	$b_b$ (mm)	$h_b$ (mm)	$b_c$ (mm)	$h_c$ (mm)	$f'_c$ (MPa)	$f_{yb}$ (MPa)	$\rho_b$	$\Gamma_N$	$V_b^{exp}$ (kN)	$v_{jh}^{exp}$ (MPa)	$p_s/\sqrt{f'_c}$	Test ID
Tsonos (2002b)	<b>O1</b>	A	200	300	200	200	16.0	485	0.010	0.25	43	3.3	0.47
	<b>O2</b>	A	200	300	200	200	16.1	485	0.010	0.25	44	3.4	0.48
Tsonos (2014)	<b>O3</b>	A	200	300	200	200	9.0	485	0.010	0.44	35	2.9	0.50
Parvin <i>et al.</i> (2010)	<b>U.S.2</b>	B	300	500	300	300	25.0	420	0.004	0.31	43	1.5	0.06
	<b>U.S.2</b>	A	300	500	300	300	25.0	420	0.006	0.31	82	2.9	0.22
	<b>U.S.3</b>	B	300	500	300	300	25.0	420	0.004	0.31	45	1.6	0.07
	<b>U.S.3</b>	A	300	500	300	300	25.0	420	0.006	0.31	84	2.9	0.23
	<b>U.S.4</b>	B	300	500	300	300	25.0	420	0.004	0.16	37	1.3	0.09
	<b>U.S.4</b>	A	300	500	300	300	25.0	420	0.006	0.16	80	2.8	0.34
Karayannis and Sirkelis (2008)	<b>A1</b>	A	200	300	200	200	36.4	574	0.003	0.05	22	2.0	0.22
	<b>A2</b>	A	200	300	200	200	36.4	574	0.003	0.05	22	1.8	0.19
Karayannis <i>et al.</i> (2008)	<b>A0</b>	A	200	300	200	200	31.6	580	0.003	0.06	24	2.0	0.23
	<b>B0</b>	A	200	300	200	300	31.6	580	0.008	0.04	58	3.2	0.48
	<b>C0</b>	A	200	300	200	300	31.6	580	0.008	0.04	64	3.6	0.54
Chalioris <i>et al.</i> (2008)	<b>JA-0</b>	A	200	300	200	300	34.0	580	0.008	0.03	65	3.6	0.52
	<b>JCa-0</b>	A	100	200	100	200	20.6	580	0.008	0.10	12	3.3	0.53
	<b>JCb-0</b>	A	100	200	100	200	23.0	580	0.012	0.10	15	4.2	0.66
Karayannis <i>et al.</i> (1998)	<b>JO</b>	A	100	200	100	200	20.8	525	0.008	0.10	14	3.9	0.65
Del Vecchio <i>et al.</i> (2014)	<b>T_C1</b>	A	300	500	300	300	12.6	470	0.007	0.20	63	2.3	0.39
	<b>T_C1</b>	A	300	500	300	300	12.6	470	0.004	0.20	52	1.9	0.30
	<b>T_C2</b>	A	300	500	300	300	16.4	470	0.007	0.20	80	3.0	0.44
	<b>T_C2</b>	A	300	500	300	300	16.4	470	0.004	0.20	65	2.4	0.31
	<b>T_C3</b>	A	300	500	300	300	16.3	470	0.007	0.20	83	3.1	0.46
	<b>T_C3</b>	A	300	500	300	300	16.3	470	0.004	0.20	70	2.6	0.35
Kaya <i>et al.</i> (2008)	<b>3</b>	A	250	500	250	250	13.5	360	0.005	0.40	28	1.4	0.11
	<b>4</b>	A	250	500	250	250	13.5	360	0.006	0.40	31	1.5	0.13
Genesio (2012)	<b>JT1-1</b>	A	300	400	350	300	25.4	554	0.007	0.00	77	3.7	0.73
	<b>JT2-1</b>	D	300	400	350	300	28.2	309	0.007	0.00	42	2.0	0.37
	<b>JT3-1</b>	B	300	400	350	300	27.5	560	0.007	0.00	38	1.8	0.35
	<b>JT4-1</b>	C	300	400	350	300	28.2	554	0.007	0.00	41	1.9	0.37
	<b>JT5-1</b>	A	300	400	350	300	28.2	540	0.004	0.00	51	2.4	0.46
Helal (2012)	<b>JA-1</b>	A	260	400	260	260	22.5	590	0.008	0.10	45	2.5	0.35
	<b>JA-2</b>	A	260	400	260	260	31.4	590	0.008	0.12	56	3.1	0.32
	<b>JA-3</b>	A	260	400	260	260	28.6	590	0.008	0.08	51	2.9	0.37
	<b>JA-4</b>	A	260	400	260	260	28.6	590	0.008	0.08	50	2.8	0.35
Liu (2006)	<b>RC-1</b>	A	200	330	230	230	19.4	324	0.007	0.07	30	2.6	0.54
Kim <i>et al.</i> (2016)	<b>EN</b>	A	350	480	350	350	20.0	550	0.012	0.00	47	2.4	0.64
	<b>EN</b>	A	350	480	350	350	20.0	550	0.006	0.00	35	1.8	0.47
Di Ludovico <i>et al.</i> (2012)	<b>T-C2</b>	A	300	500	300	300	19.2	470	0.007	0.20	77	2.9	0.35
	<b>T-C2</b>	A	300	500	300	300	19.2	470	0.004	0.20	67	2.5	0.28
Realfonzo <i>et al.</i> (2014)	<b>J-05</b>	A	300	400	300	300	14.8	540	0.010	0.23	70	3.0	0.45
	<b>J-01</b>	A	300	400	300	300	16.4	540	0.008	0.20	66	2.8	0.39
Hadi and Tran (2016)	<b>T0</b>	A	200	300	200	200	41.0	551	0.008	0.00	36	3.6	0.56
Ghobarah and Said (2001)	<b>T1</b>	A	250	400	250	400	30.8	425	0.012	0.19	115	5.1	0.53

Table B1 Continued

Test ID	Type	$b_b$ (mm)	$h_b$ (mm)	$b_c$ (mm)	$h_c$ (mm)	$f'_c$ (MPa)	$f_{yb}$ (MPa)	$\rho_b$	$\Gamma_N$	$V_b^{exp}$ (kN)	$V_{jh}^{exp}$ (MPa)	$\rho_s/\sqrt{f'_c}$	
Ha <i>et al.</i> (2013)	<b>LBCJC</b>	A	225	300	300	300	27.3	474	0.013	0.15	62	3.7	0.39
Le-Trung <i>et al.</i> (2010)	<b>NS</b>	A	134	200	167	167	36.5	324	0.012	0.00	14	3.9	0.76
Gergely (2000)	<b>1</b>	C	356	407	356	407	20.0	414	0.014	0.00	129	1.2	0.28
	<b>2</b>	C	356	407	356	407	20.0	414	0.014	0.00	142	1.4	0.31
	<b>10</b>	C	356	407	356	407	34.0	414	0.014	0.00	126	1.2	0.21
	<b>11</b>	C	356	407	356	407	34.0	414	0.014	0.00	148	1.4	0.25
Ricci <i>et al.</i> (2016)	<b>1</b>	D	300	500	300	300	28.8	344	0.008	0.10	79	3.0	0.35
	<b>2</b>	D	300	500	300	300	28.8	316	0.004	0.10	53	2.0	0.19
De Risi and Verderame (2017)	<b>1b</b>	D	300	400	300	300	17.7	370	0.010	0.10	52	2.6	0.44
	<b>2b</b>	D	300	400	300	300	17.7	330	0.007	0.10	50	2.5	0.43
	<b>1c</b>	D	300	600	300	300	17.7	370	0.007	0.10	68	2.1	0.32
	<b>2c</b>	D	300	600	300	300	17.7	330	0.004	0.10	47	1.4	0.19
Akguzel and Pampanin (2012)	<b>2DB2</b>	D	230	330	230	230	17.9	430	0.004	0.21	25	2.0	0.24
	<b>2DB2</b>	D	230	330	230	230	17.9	430	0.004	0.05	20	1.6	0.34
Pampanin <i>et al.</i> (2007)	<b>T1</b>	D	200	330	200	200	23.9	357	0.005	0.13	16	1.9	0.21
	<b>T1</b>	D	200	330	200	200	23.9	357	0.005	0.08	14	1.6	0.22
	<b>T2</b>	D	200	330	200	200	23.9	357	0.005	0.13	16	1.9	0.21
	<b>T2</b>	D	200	330	200	200	23.9	357	0.005	0.08	14	1.6	0.22
Kam (2010)	<b>NS-O1</b>	D	230	330	230	230	17.3	362	0.004	0.22	25	2.0	0.24
	<b>NS-O1</b>	D	230	330	230	230	17.3	362	0.004	0.05	19	1.6	0.34
	<b>S-O1</b>	D	230	330	230	230	15.1	335	0.004	0.24	22	1.8	0.22
	<b>S-O1</b>	D	230	330	230	230	15.1	335	0.004	0.06	19	1.5	0.33
Laterza <i>et al.</i> (2017)	<b>T23</b>	D	200	330	200	200	14.4	335	0.007	0.15	16	1.8	0.32

\*Note: <sup>a</sup> Joints with 90°-hook bent into the core; <sup>b</sup> Joints with straight anchorage into the joint core;

<sup>c</sup> Joints with 90°-hook bent out the core; <sup>d</sup> Joints with 180°-hook;

## Appendix C

See Tables C1

Table C1 Database of experimental tests on FRP strengthened joints

Test ID	Type	$f'_c$ MPa	$r_N$	$f_{yb}$ MPa	$\rho_b$	$AE^d \times 10^6$	$V_b^{exp}$ kN	$v_{jh}^{exp}$ MPa	$p_{t,tot}^e$ $exp$	$p_{t,c}^{exp}$	$p_{t,f}^{exp}$	$g_{f,e}^{exp}$	
Del Vecchio <i>et al.</i> (2014)	T_FL1	A <sup>a</sup>	13.5	0.20	470	0.007	15	73	2.9	0.50	0.36	0.15	0.0061
	T_FL1	A	13.5	0.20	470	0.004	15	63	2.5	0.40	0.29	0.11	0.0047
	T_FS1	A	17.7	0.20	470	0.007	15	106	4.2	0.66	0.33	0.33	0.0157
	T_FS1	A	17.7	0.20	470	0.004	15	85	3.4	0.49	0.26	0.22	0.0106
	T_FS2	A	16.4	0.20	470	0.007	31	123	4.9	0.87	0.34	0.53	0.0121
	T_FS2	A	16.4	0.20	470	0.004	31	95	3.7	0.61	0.27	0.34	0.0077
Di Ludovico <i>et al.</i> (2012)	T_FRP	A	14.8	0.20	470	0.007	15	100	4.0	0.72	0.35	0.37	0.0161
	T_FRP	A	14.8	0.20	470	0.004	15	78	3.1	0.50	0.28	0.22	0.0097
El-Amoury and Ghobarah (2002)	T-R1	B <sup>b</sup>	43.5	0.14	477	0.012	33	110	4.7	0.38	0.27	0.11	0.0032
	T-R2	B	39.5	0.15	477	0.012	47	115	4.8	0.43	0.27	0.16	0.0030
Gergely (2000)	4	C <sup>c</sup>	20.0	0.00	414	0.014	197	187	2.0	0.44	0.39	0.05	0.0002
	8	C	20.0	0.00	414	0.014	197	187	2.0	0.44	0.39	0.05	0.0002
	9	C	20.0	0.00	414	0.014	197	216	2.3	0.51	0.39	0.12	0.0006
	12	C	34.0	0.00	414	0.014	197	217	2.3	0.39	0.35	0.04	0.0002
	13	C	34.0	0.00	414	0.014	197	204	2.1	0.37	0.35	0.01	0.0001
	14	C	34.0	0.00	414	0.014	197	229	2.4	0.41	0.35	0.06	0.0004
Antonopoulos and Triantafillou (2003)	S63	A	19.4	0.06	585	0.008	52	40	2.9	0.55	0.49	0.06	0.0003
	S33L	A	21.0	0.05	585	0.008	33	45	3.2	0.59	0.49	0.11	0.0011
	F11	A	18.2	0.06	585	0.008	22	43	3.1	0.61	0.50	0.11	0.0016
	F22	A	21.8	0.05	585	0.008	43	50	3.6	0.67	0.48	0.18	0.0014
	F21	A	21.6	0.05	585	0.008	36	51	3.7	0.69	0.48	0.20	0.0018
	F12	A	23.6	0.05	585	0.008	28	44	3.2	0.56	0.48	0.08	0.0010
	F22A	A	22.2	0.13	585	0.008	43	57	4.2	0.63	0.43	0.20	0.0016
	F22W	A	23.4	0.05	585	0.008	43	56	4.1	0.73	0.48	0.25	0.0020
	F22in	A	16.8	0.07	585	0.008	43	42	3.1	0.62	0.50	0.12	0.0008
GL	A	15.6	0.07	585	0.008	21	44	3.2	0.68	0.50	0.18	0.0023	
Parvin <i>et al.</i> (2009)	2-RC2U1	A	25.0	0.31	420	0.006	62	130	4.9	0.56	0.22	0.34	0.0047
	3-RC3U3	A	25.0	0.31	420	0.006	148	131	4.9	0.56	0.22	0.34	0.0020
	4-RC3U3	A	25.0	0.16	420	0.006	148	135	5.1	0.83	0.30	0.52	0.0031
	2-RC2U1	B	25.0	0.31	420	0.004	62	85	3.2	0.27	0.09	0.18	0.0025
	3-RC3U3	B	25.0	0.31	420	0.004	148	99	3.7	0.35	0.09	0.26	0.0015
	4-RC3U3	B	25.0	0.16	420	0.004	148	89	3.3	0.45	0.14	0.31	0.0018
Garcia <i>et al.</i> (2013)	JA2RF	A	54.2	0.04	551	0.008	98	86	4.9	0.53	0.38	0.15	0.0014
	JB2RFb	A	55.3	0.04	551	0.008	128	120	6.8	0.78	0.38	0.40	0.0029
	JC2RF	A	56.9	0.04	551	0.008	128	119	6.8	0.77	0.38	0.39	0.0028
Shrestha <i>et al.</i> (2009)	SC1	A	25.8	0.08	532	0.013	1	98	3.8	0.57	0.52	0.05	0.0451
Realfonzo <i>et al.</i> (2014)	J-02	A	19.5	0.17	540	0.008	41	81	3.6	0.53	0.44	0.09	0.0014
Ha <i>et al.</i> (2013)	J-CS1	A	27.3	0.15	474	0.013	19	70	3.8	0.49	0.36	0.13	0.0040

\*Note: <sup>a</sup> Joints with 90°-hook bent into the core; <sup>b</sup> Joints with straight anchorage into the joint core;<sup>c</sup> Joints with 90°-hook bent out the core; <sup>d</sup>  $AE = A_{f,eq} \times E_f$ ; <sup>e</sup>  $p_t / \sqrt{f'_c}$  (MPa<sup>0.5</sup>)